POLYMERS FOR REVERSIBLE CELL ENCAPSULATION

To my parents, Fathiyeh Ehteshami and Firooz Mohajeri

AND

To my husband, Behnam Naderizand

POLYMERS FOR REVERSIBLE CELL ENCAPSULATION

By

Sara Mohajeri, B.ENG

A Thesis

Submitted to the School of Graduate Studies

In Partial Fulfillment of the Requirements

For the Degree

Masters of Science

McMaster University

MASTER OF SCIENCE (2011) McMaster University

(Chemistry) Hamilton, Ontario

TITLE: Polymers for Reversible Cell Encapsulation

AUTHOR: Sara Mohajeri,

B.Eng. (Amirkabir University of Technology, Iran)

SUPERVISOR: Dr. Harald D. H. Stöver

NUMBER OF PAGES: 91

ABSTRACT

Cell encapsulation aims to introduce immune-isolated living cells into patients to treat endocrine disorders. The conventional microcapsule structure is the alginate/PLL/alginate capsule (APA), which can provide a fairly biocompatible, semi-permeable shell for cells, but with insufficient chemical-mechanical stability. Clinical applications of APA capsules are still far off due to PLL protein absorption, alginate cytotoxicity and weakening the interpenetrated porous structure through the sodium/ calcium ion exchange.

In this study, a reactive polyanion (poly (methacrylic acid-*co*-2[methacryloyloxy] ethyl acetoacetate), 70:30, A70) was prepared by free radical polymerization in ethanol. A70 was combined with sodium alginate solution, and gelled in calcium chloride to provide crosslinked shell around PLL-coated CaAlg capsules, and to reinforce the CaAlg core by forming covalent bonds with PLL that diffused to the capsule interior.

This system benefits from a rapid non-toxic crosslinking reaction at physiological conditions. The mechanism and rate of covalent bond formation and cleavage were studied with the help of model reactions and UV/Vis and ^{1}H-NMR. We also studied the ability of polyanion, A70, to reinforce the CaAlg core by forming covalent bonds with in-diffused PLL. The PLL diffusion depth, the mobility of A70 inside the CaAlg gel, the encapsulation process and microcapsule structure were studied in detail. Network degradation was also studied using gel dissolution for the capsules stored at 37°C, and correlated with studies of chemical hydrolysis of the network forming polyanion.

Overall, this thesis introduces a simple, fast and accurate method to study the polyelectrolyte ability to form enamine bonds, and the stability of resulting crosslink bond in aqueous solution via small molecule models with an acceptable match to real microcapsules. According to these results the synthetic polyanion, A70, showed significant potential for applications that require protection of cells for the time needed to develop their own extracellular matrix, and as such can certainly find valuable uses in the field of cell encapsulation.

ACKNOWLEDGEMENTS

In the first place, I would like to express my deep appreciation to my supervisor Professor Harald D. H. Stöver for his instruction and constant encouragement during the whole period of my research. His knowledge, motivation and patient helped me to learn so much about chemistry and scientific concepts. I greatly appreciate him for everything.

I would like to thank my committee member, Dr. Todd R. Hoare from the Faculty of Chemical Engineering for his knowledge and suggestions to keep my project in the right direction.

I would also like to express special thanks to Dr. Nicholas A. D. Burke for his kind help and support over the past few years. I believe this thesis would not have been completed without his experience and knowledge.

I am grateful to my research group: Dr. Jian (Jeffrey) Li, Dr. Jafar Mazumder, Casey Gardner, Padraic Foley, and Rachelle Kleinberger. I would also like to thank Dr. Bob Berno from NMR facility, Marcia Reid and Marine Timleck from Electron Microscopy in the Faculty of Health Sciences, and Dr. Adronov's group for using UV/Vis spectrometer.

I would like to express my special thanks to my husband Behnam Naderizand for his love, patience and support over the past eight years and especially during these challenging two years living far from our lovely country, IRAN. I would not be able to succeed without his sacrifice and encouragement. My mother Fathiyeh Ehteshami and my father Firooz Mohajeri, without them and without their inspiration, support and love I would never exist and be who I am. I really appreciate them for respecting my decision to leave them and continue my education far from my hometown. My sisters, Parisa and Leila, for the times being together and their love and encouragement. I dedicated this work to all of them.

I would like to appreciate my beautiful lovely country IRAN for everything it has offered me to make my life and future. I hope one day I come back home and compensate all its unsparing generosity.

Finally, thank GOD for past, now, and future.

TABLE OF CONTENTS

Chapter 2: Model Studies of Enamine Formation from Acetoacetates and Amines

Chapter 3: Core Crosslinked Alginate Microcapsule

LIST OF FIGURES

LIST OF SCHEMES

Chapter 1: Introduction to Cell Encapsulation

1.1 Aim of the Thesis

To study the chemical properties of a reactive polyanion formed by copolymerization of 70 mole% methacrylic acid with 30 mole percent methacryloylethylacetoacetate, and used to reinforce calcium alginate capsules in cell encapsulation applications. Such capsules are potentially useful to treat Parkinson, Alzheimer, diabetes, hemophilia and other metabolic disorders. This thesis focuses on the polyanion reactivity and ability to form covalent crosslinks with poly-L-lysines, the stability of these covalent crosslinks, and its application on forming core-crosslinked capsules.

1.2 Cell Encapsulation

The inability of the body to produce essential enzymes or hormones is the cause of many diseases. Cell therapy aims to introduce living cells into patients to treat metabolic disorders such as Parkinson, Alzheimers, diabetes, liver failure, hemophilia etc. Cell therapy often focuses on the implantation of autologous or allogeneic cells into the patient. However, the immune response from the patient to the allogeneic cells, as well as low availability of donor tissue, severely limits the cell therapy application. [1, 2] To prevent the immune response and develop functional cell therapies, physical immunoisolation of cells was proposed to protect autologous cells from the immune system within devices fabricated from biocompatible materials, without immunosuppressant drugs.[3] The encapsulation concept for the immunoprotection of transplanted cells was introduced for the first time in 1960s by T.M.S Chang as a Ph.D. thesis in McGill University.[2] The cell encapsulation method produces a selectively permeable membrane containing cells that allow in-diffusion of essential molecules such as nutrients, oxygen, and growth factors for

cell metabolism, as well as out-diffusion of waste products and therapeutic proteins (Figure 1.1). Moreover, cells and larger molecules of the immune system are kept out, avoiding the need for cytotoxic immunosuppressant drugs. [4, 5]

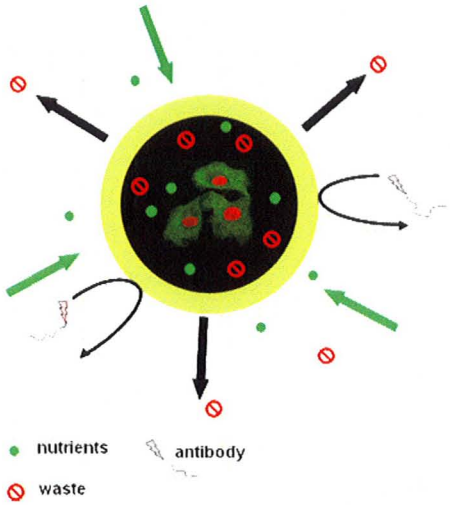

Figure 1.1 Concept of cell immunoisolation in microcapsules.

Encapsulation of cells allows for extended, continuous delivery of drug expressed by these cells, and may enable biofeedback to regulate drug delivery, such as in diabetes. Moreover, it is possible to transplant xenogeneic cells and express any desired protein *in vivo* without any modification of the host's genome.[6]

To achieve these aims different cell encapsulation devices have been designed.

1.3 Encapsulation Techniques

Different macro and micro scale device types have been proposed to encapsulate cells. For all devices, an optimal balance has to be maintained among parameters such as mass transfer, biocompatibility, and cell proliferation space to provide suitable condition for drug production and release. The macroencapsulation devices such as intravascular

tubular implants, hollow fibers, and flat disk-shaped implants allowed the implantation of large amount of cells with acceptable host immune responses.[2] Macrocapsules have the advantage of easy implantation and retrievability.[7] However, the low surface/volume ratio cannot provide essential mass transfer properties,[8] and decreases the cell functionality and viability. For example, several meters of hollow fibers are required to implant sufficient pancreatic tissue and control the blood glucose level in the treatment of diabetes.[9]

In contrast, microcapsules (0.3-1.5 mm diameter range[10]) showed significant advantages for cell transplantation. Several studies showed that mass transfer is optimized by the extremely high surface vs. volume ratio which is critical for cell viability, fast secretory response to external signal and rapid equilibrium of permanent molecules.[2, 11] In fact, small size capsules have higher surface to volume ratio increases good transport of essential nutrients and higher stability.[12, 13]Low diffusion rate of essential materials can lead to cell death, decrease the drug producing rate, and release antigens in the environment inducing immune response.[14]Although microcapsules are not connected to the unhealthy organ as an artificial device, they support entrapped cell metabolism, growth, and differentiation.[10]

Depending on the choice of microcapsule material and on whether the membrane was pre-fabricated or is formed around the viable cells, different parameters should be considered for the design of a microencapsulation device. The mass transport properties of the microcapsule are critical since the microcapsules should be semi-permeable to permit entry of nutrients and exit of waste material, and immuno-isolate cells by excluding other cells as well as antibodies and certain cytokines.[5, 6] The metabolic requirements of various cell types are different, hence, the microcapsule permeability depends on the choice of cells, and the molecular mass cut-off (MWCO) will be application dependent. For well controlled transport properties, it is obligatory to make small microcapsules with uniform wall thickness. The small size microcapsules (100-500μm) not only provide a large surface/volume ratio which improves mass transport properties, but also allow their implantation in close contact to the blood stream and

possibly formation of a vascular network surrounding the microcapsule. The vascular network provides essential supply of nutrition and oxygen for the entrapped cells, enhancing the long-term functionality of the microcapsule (Figure 1.2).[6] Besides permeability, the availability of extracellular matrix (ECM) to encapsulate cells, especially for anchorage dependent cells is another important consideration.[15, 16]

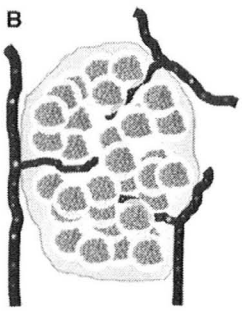

Figure 1.2 The formation of vascular network surrounding a microcapsule network.[6]

Moreover, implanted microcapsules must resist physical and biochemical stress to prevent breakage of the capsule and immune rejection of the encapsulated cells. The ideal capsule shell and core degradation rate depends on the kind of cells and the application. Some cells may benefit from remodeling or degradation of their immediate extracellular matrix, while in many cases permanent shells may be desirable. The other important character for fabricating suitable microcapsule is the biocompatibility of the initial capsule material and by-products towards both cells and host, that is not be toxic to either and not elicit an immune response from the host.

According to these essential properties different microcapsule structure (section 1.2), polymeric structure (section 1.3), and preparation methods (section 1.4) were proposed to form microcapsules.

1.4 Microcapsule Structure

Microcapsules are classified in three categories: matrix-core/shell microcapsules where cells are embedded in hydrogel matrix, liquid-core/shell microcapsules where cells are suspended in a liquid core and conformal microcapsules which individual cells or cell clusters are coated directly (Figure 1.3).[15]

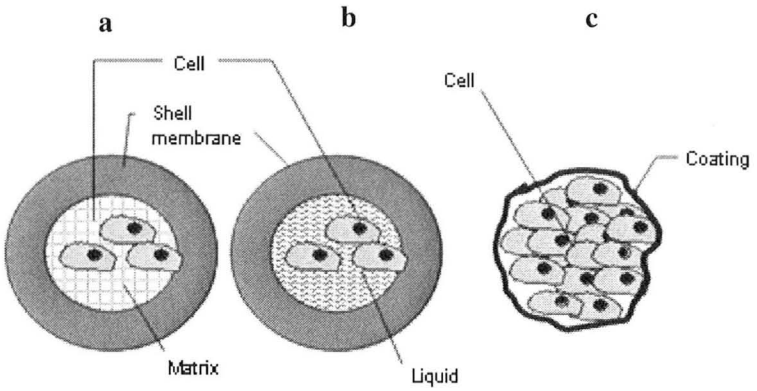

Figure 1.3 Microcapsule Structure: a) Matrix-core/shell microcapsules; b) Liquid-core/shell microcapsules; c) conformal microcapsules.[12]

Matrix-core/shell microcapsules are the most popular structure for cell encapsulation of anchorage dependent cells. In this method cells are embedded in a hydrogel, i.e. a network of hydrophilic polymer, which can be designed with different covalent and/or non-covalent crosslinking methods compatible with cell viability.[17, 18]

Embedding cells in hydrogels has several advantages as cells are retained in an aqueous environment in contact with soft biocompatible materials which protect them from the stress of encapsulation. Also the hydrogel can be a reversible structure which disintegrates in response to changes in temperature, pH, and salt concentration.[12]

1.5 Methods of Hydrogel Bead Formation

Cell encapsulation in hydrogel requires microcapsules formed by cell compatible, economical and reproducible method such as emulsification, extrusion and

co-extrusion. The microcapsule generation methods are limited by physical factors such as high viscosity of the bead making solution, size and size distribution, and the mechanical strength of the resulting microcapsule.[19]The important challenge is producing uniform small size capsules (100-500 μm) with a smooth surface to optimize mass transfer. In this part some common cell encapsulation methods will be described.

1.5.1 Emulsion Method

In this technique the aqueous solution is mixed and dispersed in an immiscible organic phase such as a vegetable oil, and often facilitated by surfactants. After the equilibrium dispersion is reached, gels are formed by cooling or by adding a gelling agent into the emulsion. After hardening the hydrogel, capsules are separated and washed in water or saline as appropriate (Figure 1.4).

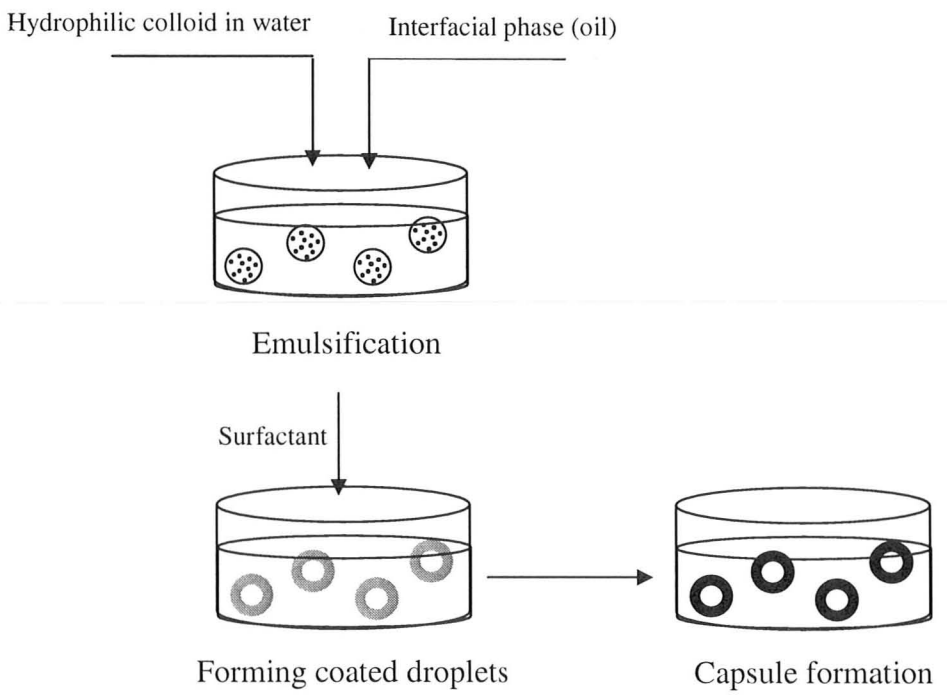

Figure 1.4 Schematic scheme of emulsion method.

Although this method has some advantages for industrial purpose and can be easily scaled-up, but the large diameter, wide size distribution, and insolubility of some gelling agents such as calcium chloride ion for alginate gel formation[20, 21] besides the shear stress to cells that leads to heterogeneous cell distribution within the capsule currently still limits the applications of emulsion method.

1.5.2 Extrusion Method

In this technique, the crosslinkable polymer solution containing cells is extruded through a small tube or needle. The droplet falls into a hardening bath and the polymer is crosslinked by an appropriate reagent such as divalent cation, polyelectrolyte, cooling, and etc (Figure 1.5).

The simplest extrusion system consists of a dripping mode with pressure as the driving force. Its applications are limited to low viscosity solution and production of large bead sizes (0.5-3 mm). Smaller capsules can be obtained by smaller dripping needles, lower polymer concentration, viscosity, or lower flow rate, but still high viscosity polymers are preferred to give stronger and less permeable capsules.[22]

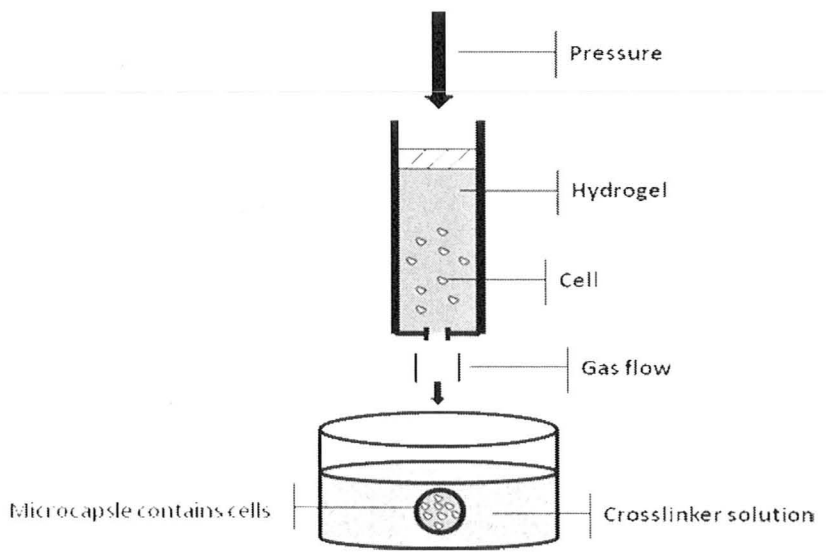

Figure 1.5 Schematic scheme of extrusion method.

To decrease the capsule size an extrusion technique aided by coaxial gas flow is often utilized. In this method, the compressed gas flows around the tip of the extrusion nozzle shears the droplets, and controlling their size. While this method has a fairly low rate of capsule formation, but it is suitable for high viscosity polymers, [22, 23] and small size capsules around 150μm can be obtained by micro-airflow nozzle.[24]

1.5.3 Co-extrusion Method

In this technique a double-nozzle is used to co-extrude an aqueous polymer solution with cells via the internal nozzle, and the shell-forming solution via the external nozzle. Therefore, the resulted capsules are already coated by a shell or membrane. This technique could be interesting to make capsules immediately coated with a shell of different polymers, but it is mostly used to produce liquid-core capsules.[11]

However extrusion method is a very common method, but it has some deficiencies. The capsule size range is limited by nozzle diameter as well as viscosity of the solution and air flow, thus it is difficult to form beads with diameters of much less than 500μm. Also, this technique is not suitable for industrial scale-up due to requirements of a large number of nozzles operating simultaneously.[11] Other methods for bead formation are also being explored, including electrostatic droplet generation. In this technique a high-voltage electrostatic pulse was applied for producing small alginate beads (<300 μm). [25-27]

1.6 Matrix-core/shell Microcapsule Material

The microcapsule material should cover several essential parameters to form a suitable device for cell encapsulation includes: biocompatibility, sterilizability, lack of toxic material or temperature need for synthesis or crosslinking, long term biostability, suitable degradation time if desired, and ease of processing into beads. The microcapsule materials also directly affect the mass transport properties and morphology. For this purpose, different biomaterials with different gel formation mechanisms were explored.

1.6.1 Thermal Hydrogel

One of the common natural materials for cell encapsulation is agarose, a temperature-dependent hydrogel, with fast gelation in aqueous solution leading to strong porous capsules even at low polymer concentration (0.2%).[28]It is a polymer of alternating units of β-D-galactopyranose and 3, 6-anhydro-α-D-galactopyranose (Figure 1.6).

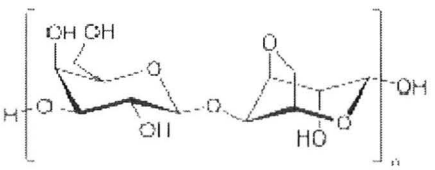

Figure 1.6 Chemical structure of agarose.

These capsules are usually produced by a one-step extrusion method[29] or by a water-oil emulsion technique.[30-32] The properties of the resulting agarose capsule depend on MW, MW distribution, content of charged groups and monomer distribution.[31, 33] Previous studies revealed that the cell viability in agarose capsules decreased at agarose concentrations below 7.5%, in studies of transplantation of xenograft islets.[34]. Mixing agarose with other polymers such as polystyrene sulfonic acid.[35, 36] or polyvinyl sulphate[37] increases xenograft survival time.

The agarose/collagen blend is the most common mixture which improves the cell viability in capsules by surrounding the cells with a small amount of a physiological relevant matrix.[38, 39] Also, thermally-gelable synthetic polymers such as poly (N-isopropyl acrylamide) (PNIPAAm) and its copolymers with PEG, PNIPAAm-PEG-PNIPAAm, showed valuable gel formation at physiological temperature. The resulting capsules revealed suitable mechanical stability, high cell viability and no toxicity under physiological conditions.[40]

1.6.2 Ionotropic Hydrogel

The inner structure of matrix-core capsules is often an ionotropic gel, typically formed from polyelectrolytes (PE) crosslinked spontaneously with divalent cations or, less commonly, anions. The gel structure depends on polyelectrolyte properties such as molecular weight (MW), density, architecture, nature of the charge and also on the crosslinking ions. Alginate is the most common ionotropic cell embedding material which is a negatively-charged, linear polysaccharide (PS) copolymer of 1, 4-linked β-D-mannuronic acid (M) and α-L-guluronic acid (G) which extracted from brown seaweed for the first time in 1881 by E.C. Stanford. The monomer units arranged in mannuronic and guluronic blocks (MM, GG), or alternating sequences (MG block) (Figure 1.7). Alginate forms a three dimensional interconnected network at room temperature or any other temperature up to 100°C in the presence of divalent cations such as calcium,[41] barium[42] and strontium[43] which does not melt when heated.

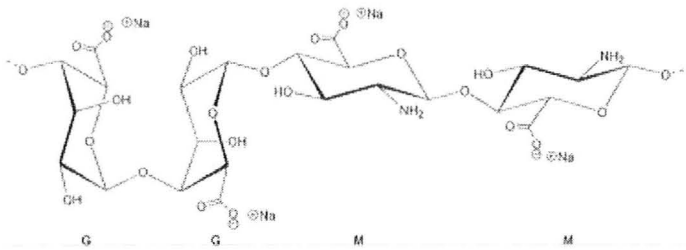

Figure 1.7 Chemical structure of sodium alginate.

In this mechanism, alginate mainly crosslinks and forms gel structure by the exchange of sodium ions from the guluronic acids with the divalent cations, mostly calcium ions, and then the crosslinked groups arrange to form the so-called egg-box structure (Figure 1.8).[44, 45]

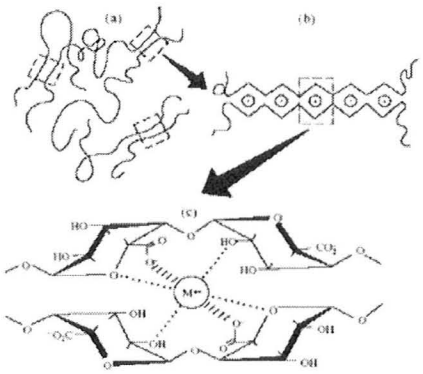

Figure 1.8 "Schematic representation of the "egg-box" model of alginate gel. (a, b) Binding zones between polymeric alginate molecules; (c) an elementary cell of the binding zone. The dotted line indicates hydrogen bonds between the oxygen atoms of the pyranosic cycles and the metallic ion; the dashed line indicates ionic bonds between carboxyl groups and the metallic ion (adapted from McHugh et al; 1987)".[46]

In this structure, the divalent ion is ionically substituted at the carboxylic site. A second alginate strand can also connect at the calcium ion, forming a link in which the divalent ion attaches two alginate strands together. "The analogy is that the strength and selectivity of cooperative binding is determined by the comfort with which 'eggs' of the particular size may pack in the 'box', and with which the layers of the box pack with each other around the eggs" (Grant et al., 1973). This model can form a three-dimensional network as the polymeric structure. Also polymer chain aggregates bind the calcium ions more firmly which is called "cooperative binding". In fact, the configuration of guluronic acid chains provides a distance between carboxyl and hydroxyl groups which allows an effective interaction with calcium.

According to alginate chemical structure and gel formation mechanism, different parameters affect the alginate capsule:

A. Effect of Alginate Structure on Alginate Gel Formation

In the alginate hydrogels, the G/M ratio can affect several properties such as gel strength, gel permeability, and biocompatibility.[47-49] The alternate sequence (MG block) is more flexible and provides for a less viscous solution whereas the guluronic blocks (GG) are stiffer and more viscous in solution, but form more stable gels and rounder particles. These resulting beads showed higher mechanical stability and are more resistant to swelling caused by osmotic pressure. Therefore, in cell encapsulation alginate with a high content of guluronic acid blocks is more desirable. Also this kind of alginate provides highly transparent beads which are suitable for encapsulating photosynthesizing cells. In contrast, for applications where recovery of the cells is essential, alginate with a lower content of guluronic blocks which forms softer and more flexible gels is required to dissociate the gel more easily.[47, 50]

It is further possible to optimize the osmotic swelling, permeability and gel strength by changing the alginate MW.[51] However, the application of high MW alginate is limited due to high viscosity producing more irregular surfaces and bigger capsules.

B. Effect of divalent ion on Alginate Gel Formation

Alginate has shown decreasing binding affinities for different divalent ions: Pb > Cu > Cd > Ba > Sr > Ca > Co, Ni, Zn> Mn. Traditionally calcium is widely used to crosslink alginate, but calcium-alginate beads are sensitive toward chelating agents such as phosphate and citrate. Calcium ions also are easily replaced over time by nongelling agents such as sodium in saline solution. The resulting osmotic swelling of the beads in physiological solution leading to dissociation of ionic bridges, bigger pores, shorter degradation time and lower mechanical stability. To increase the stability of the beads, barium alginate beads were used by many groups which form stronger beads due to higher alginate affinity to divalent ion. This kind of beads also showed more heterogeneous alginate gel distribution that does not change through washing and coating steps. In fact inhomogeneity is the result of a rapid irreversible gelling mechanism by a strong site binding of barium ions to alginate chains, and it is a more favourite microcapsule structure due to low permeability.[42, 52-54]

1.7 Alginate Capsule Structure

1.7.1 Alginate Capsule Coated by Polyelectrolyte Complex Gel

The most frequently employed method to improve mechanical strength, and extend the alginate gel degradation time is by forming a polyelectrolyte complex (PEC) gel around calcium alginate capsules. This complexation is driven by the interaction between two oppositely charged water soluble polymers, polyanion and polycation, to form a complex coacervate as a separate phase. This complex contains less water and more polymer than the initial solutions, and can be insoluble in water or other common solvents. The PEC nature and the possible chemical reactions and physical interactions depend on such variables as degree of dissociation of the polyelectrolytes, the nature and position of ionic groups on polymeric chains, polyelectrolyte concentration, molecular weight and flexibility of polymeric chains, mixing ratio, mixing order, the duration of interaction as well as temperature, pH, and ionic strength of the solution phase.[55, 56]

In this approach, the alginate capsule containing cells are coated with a solution of polycation to form a polyelectrolyte complex on the capsule surface. This process has some resemblance to the layer-by-layer assembly introduced by Decher and co-workers in 1992 to prepare controlled structure thin films for biological applications.[57] Decher's method is based on alternating immersion of substrate into dilute solutions of oppositely charged polyelectrolytes to produce multilayers on the surface (Figure 1.9). Since a single bilayer of polyelectrolyte bound to a smooth hard surface can be as thin as 1 nm or less, the LBL technique allows excellent control of film thickness on hard smooth substrates.[58-60]

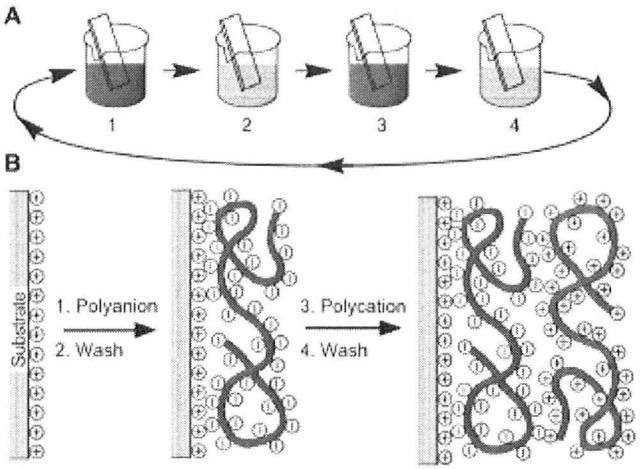

Figure 1.9. "(A) Schematic of the film deposition process using slides and beakers. Steps 1 and 3 represent the adsorption of a polyanion and polycation, respectively, and steps 2 and 4 are washing steps. The four steps are the basic buildup sequence for the simplest film architecture, $(A/B)_n$. (B) Simplified molecular picture of the first two adsorption steps, depicting film deposition starting with a positively charged substrate. The polyion conformation and layer interpenetration are an idealization of the surface charge reversal with each adsorption step."[59]

Coating of calcium alginate hydrogels by the LbL process has important differences form Dechers approach, as hydrogels are highly porous and hence lead to PEC layers with substantial thicknesses of many micrometers. According to LBL method, the coated alginate capsules contain layers held together by the electrostatic interaction between oppositely charged polymers. The polyelectrolyte structure and MW control the polyelectrolyte complex gelling properties as well as capsule density, permeability and mechanical stability. An important factor in this technique is the isolation of cells from toxic polycations to maintain their viability, ability to grow and divide inside the capsule. The most commonly used polycation for cell encapsulation is poly (L- Lysine) (PLL) as originally described by Lim and Sum in 1980 to form alginate/PLL/alginate capsules (APA) for treatment of diabetes (Figure 1.10).[61]

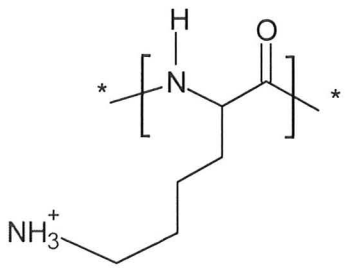

Figure 1.10 Chemical structure of Poly (L-Lysine).

In this structure, PLL interacts with negative charges on and near the surface of alginate capsules (Figure 1.11).

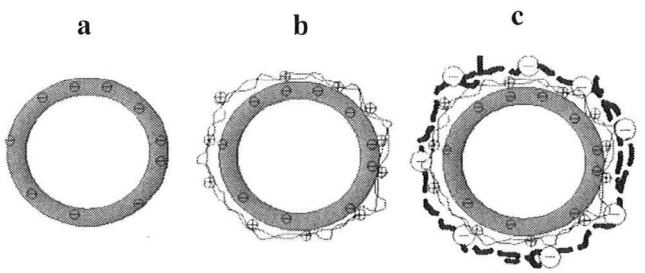

Figure 1.11 Multilayer polyelectrolyte coating on alginate microcapsule: a) Alginate microcapsule; b) PLL (polycation) deposition; c) Alginate deposition (polyanion).[11]

PLL binding and diffusion not only depend on PLL MW, but also on the guluronic content of alginate and on the type and concentration of the divalent ion. In fact, stronger interaction between alginate and divalent ion decrease the chance of PLL to interact with alginate and diffuse into the inner layers of alginate to form complex gel. Also PLL is very susceptible to protein absorption and consequently cell overgrowth. So it is usually considered mandatory to cover the PLL layer with another layer of alginate. Previous studies showed that the high-G capsules coated by PLL result in stronger inflammatory response than intermediate-G capsules due to inappropriately PLL binding

to the high-G alginate core. In fact, in high-G capsules lower numbers of binding sites are available for PLL, and the capsules are less permeable. Thus, PLL will bind less strongly to the alginate.[62-64]

While some previous studies reported successful long-term implantation of microencapsulated allografts in APA capsules for spontaneous diabetic dogs[65] and humans,[66] clinical application are still far off due to alginate cytotoxicity and PLL protein absorption, amongst other problems. PLL has been reported to be toxic towards different cell lines by activating complement and macrophages producing interleukin-1 (IL-1) and inducing fibrosis.[67-70] Studying the surface chemical composition of APA capsules revealed that calcium alginate core is covered by a single layer membrane wherein alginate and PLL are interacting to form PEC complex. In fact, PLL is uniformly distributed among the capsule surface, and a distinct outer layer alginate does not exist.[70] Also, PEC complex gel gradually weakens overtime, exposing more accessible PLL chains to the host.[50] On the other hand, alginate has been shown to degrade during purification[71] and when exposed to biological environments,[72, 73] hence the polyelectrolyte complex gel has showed much shorter lifetime in the presence of cells[74] and exposes toxic polycation layer to immune system. As well, alginate biocompatibility depends on the source and processing as it contains variable amounts of impurities such as endotoxin, protein and polyphenols which can be reduced but not completely removed during purification.[70, 75, 76]

To increase the biocompatibility of APA capsules, PEG-grafted poly (L-Lysine) was studied[77] which decreases the protein absorption and consequently omits the extra alginate layer. However, the weakening of PEC complex due to the added PEG chains still limits their application. To overcome this inability and form more stable/stronger beads other methods were introduced to form covalently crosslinked bonds on outer the layer and/or inside the alginate capsules as described in the next sections.

1.7.2 Covalently Crosslinked Alginate Capsule

Several studies showed that forming covalent bonds in alginate capsules makes them more resistant to mechanical and chemical challenges. In this approach different chemical and photochemical crosslinking reactions were applied under physiological conditions, while considering chemical properties of materials such as cytotoxicity of crosslinking reagents, photochemical or thermal initiators, catalysts, byproducts, and residual reactive groups.

According to these parameters, different polymeric systems are suggested to make crosslinked capsules under physiological conditions. One approach is forming functionalized alginate by the chemical introduction of reactive groups such as thiol, [78-801] methacrylate and acrylate[81-84] on the alginate backbone. The functionalized alginate capsules are crosslinked by exposure to a second polymer, catalyst or light; however, applications are limited by the interfering functional group on the alginate gel. In fact, the lack of selectivity during chemical modification that generally occurs on both guluronic acid (G) and mannuronic acid (M) prevents forming alginate gel instantaneously in divalent ion bath that hence affects its application for cell encapsulation.[83, 84]

The other approach to prevent APA toxicity and produce stronger crosslinked alginate capsule is forming covalent bonds by in-diffusion of polymeric or monomeric species followed by crosslinking or polymerization. Several groups attempt to improve the strength of alginate based gels using Michael addition between thiol and acrylate end chains of pluronics polymers,[85] photodimerization of modified poly(allylamine),[86] or by the reaction between amine and ester, aldehyde/ketone, isocyanate/isothiocyanate, and thioester. [87,88] Recently, we developed synthetic polyanions containing acetoacetate group, poly (methacrylic acid, sodium salt-*co*-2-[methacryloyloxy] ethyl acetoacetate) (70:30 mol%, A70), to form a tough crosslinked shell around PLL-coated alginate beads, and to reinforce the alginate core by forming covalent bonds with interior PLL and other polyamines.[89-91] This approach is based on electrostatic attraction and preconcentration of

the reactive polyelectrolytes with subsequent covalent crosslinking in the absence of light, catalyst or initiator.

The purpose of this thesis is to study the possible chemical reactions of acetoacetate group and the stability of the formed covalent bonds, using real and model conditions. In particular, I plan to employ small molecule models and study the effect of electrostatic attraction on the reaction rate, and the covalent bond stability at different temperature and solvent.

The reaction between acetoacetate and amine will be studied by the reaction between methyl acetoacetate (MAcAc) and 3-methoxypropylamine (MOPA) as small molecule models, polyanion (A70) and MOPA as polymer-small molecule model, and between polyanion (A70) and low molecular weight PLL, as polymer-polymer models.

The ability of the crosslinking system to form core-crosslinked capsules will also be further studied, and study the long-term stability of crosslinked networks formed. Several groups reported extruding the cell containing alginate solution with concentric airflow into the gelling bath as a successful method to entrap cells in the capsule. In this approach, calcium alginate beads can be coated with PLL and polyanion (A70) via the LBL method to strengthen the surrounding gel with electrostatic attraction and covalent bonds. In order to improve the mechanical stability and degradation time of the alginate core, a mixture of alginate/reactive polyanion can be used to form primary calcium alginate capsules, followed by crosslinking of the distributed polyanion by in-diffusing PLL during the coating step. According to this method, core-crosslinked capsules can be formed depending on PLL molecular weight, polyanion mobility in alginate core, reactivity of functional groups and stability of covalent bonds under physiological conditions.

As the formation and properties of core-crosslinked capsules depend on several parameters, we aim to be able to balance these variations to achieve a covalently crosslinked core surrounded by semipermeable crosslinked shell with improved mechanical and biochemical resistance that would allow for long-term cell encapsulation.

1.8 Research Objectives

The objects of this thesis are:

1. To study the hydrolysis rate of acetoacetate as the functional group of A70, and its possible chemical reactions via model reactions.
2. To study the use of polyelectrolytes in the formation of core-crosslinked alginate capsules, including the effect of molecular weight and concentration of polyelectrolytes, on the location of these polyelectrolytes within the capsules.
3. To study the initial and long term stability of covalent bonds under physiological conditions via the molecular model and capsules.
4. To study the effect of alginate type on polyelectrolyte diffusion and mobility.

Chapter 2: Model Studies of Enamine Formation from Acetoacetates and Amines

2.1 Abstract

A random copolymer (poly (methacrylic acid-*co*-2-[methacryloyloxy] ethyl acetoacetate), 70:30, A70) was prepared by free radical polymerization in ethanol. Its hydrolysis in water at 20°C and 40°C was measured, and found to reach 42 and 83% after 32 days, respectively. As well, the rate and equilibrium position of formation of enamine between A70 and PLL was studied with the help of molecule models (small molecule model, polymer-small molecule model, and polymer-polymer model) in organic and aqueous environment, and followed by UV/Vis and ^{1}H-NMR. Our study in organic environment (DMSO) showed the enamine bond level is enhanced by increasing the concentration of reagents and acid catalysis. The reaction in aqueous environment showed low enamine formation for small molecule models which is shifted to higher equilibrium position for polymer-polymer model significantly. However, the covalent bonds slowly but permanently cleaved at physiological pH due to continuous hydrolysis of A70 at elevated temperature.

2.2 Introduction

The most frequently employed method to improve mechanical strength and lifetime of alginate-based microcapsules is to form a polycation/alginate polyelectrolyte complex (PEC) around or within the primary calcium alginate capsules. Currently, the most commonly used polycation for this purpose is poly(L-Lysine) (PLL), using a procedure originally described by Lim and Sum in 1980 to form alginate/PLL/alginate capsules (APA) encapsulating islets of Langerhans.[61] In this structure, PLL interacts with negative charges on and near the surface of alginate capsules.

While some previous studies reported successful long-term implantation of microencapsulated allografts in APA capsules for spontaneously diabetic dogs, and humans,[65, 66] clinical applications are still far off due to immune responses attributed to factors such as alginate cytotoxicity and binding of proteins by PLL, amongst other problems. Previous studies showed that the PEC complex formed at the capsule surface gradually weakens over time, exposing more accessible PLL chains to the host.[50] As well, alginate has been shown to degrade during purification[71] and when exposed to biological environments,[72, 73] hence the PLL-alginate polyelectrolyte complex gel has shown much shorter lifetime in the presence of cells, which again may lead to capsule degradation and expose the toxic polycation to the host immune system.[74] Alginate biocompatibility also depends on its source and processing, as it contains variable amounts of impurities such as endotoxins, proteins and polyphenols, which can be reduced but not completely removed during purification.[75-77] A method that might address some of these challenges is coating the PLL layer with less toxic synthetic polyanions containing reactive groups able to form a covalently bonded network around or within the capsule. In fact, the combination of covalent and electrostatic network formation should extend the degradation time of the coating layer, and the use of synthetic polymers free of biological impurities could help reduce the innate immune response.

Recently, our group developed synthetic polyanions containing acetoacetate, poly(methacrylic acid-*co*-2-[methacryloyloxy] ethyl acetoacetate) (70:30 mol%, A70)

(Scheme 2.1), designed to form a tough crosslinked shell around polyamine-coated alginate beads, and to reinforce the alginate core by forming covalent bonds with PLL that diffused to the capsule interior.[89-91] This approach is based on electrostatic attraction and preconcentration of the reactive polyelectrolytes with subsequent spontaneous covalent crosslinking without need for light, catalysts or initiators.

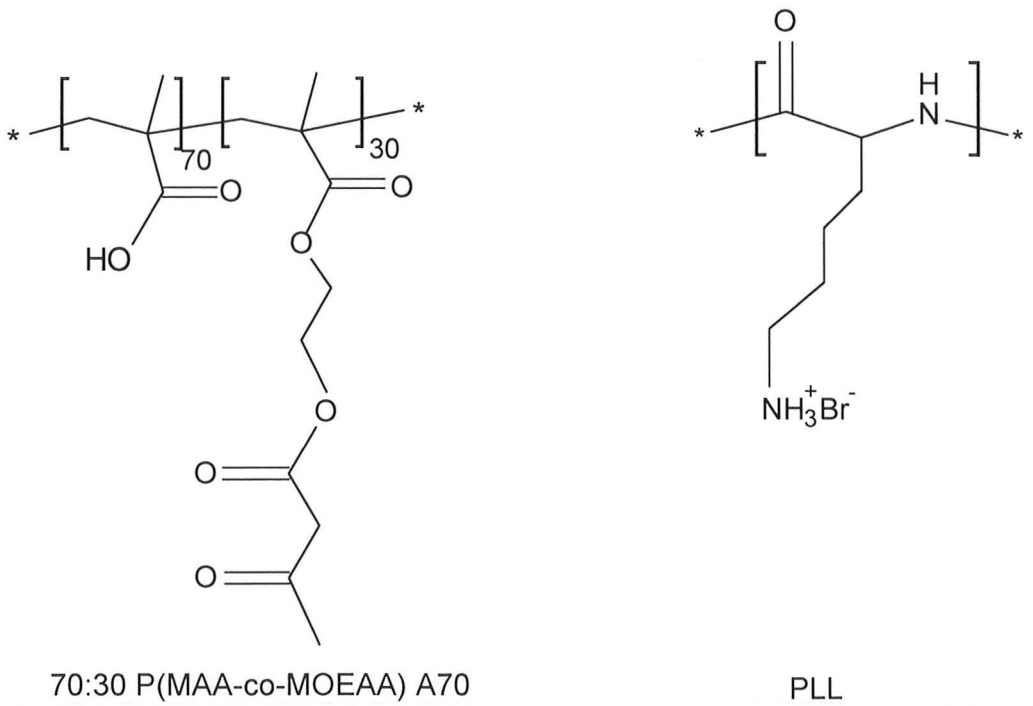

70:30 P(MAA-co-MOEAA) A70 PLL

Scheme 2.1 Structures of the synthetic polyanion, A70, and of poly-(L-Lysine), PLL.

There is some evidence based on small molecule systems that enamine formation between amine and acetoacetate in aqueous media is reversible, especially in acidic and basic solutions (Scheme 2.2.A).[92-96] Also, the acetoacetate ester has been reported to hydrolyze in other MOEAA-containing systems, which here would form hydroxyethyl methacrylate (HEMA) units and a β-keto acid and result in loss of the reactive group of A70 (Scheme 2.2.B). However, transforming the acetoacetate groups of MOEAA-

containing polymers into enamines has been reported to reduce the rate of hydrolysis of the ester group (Scheme 2.2.C).

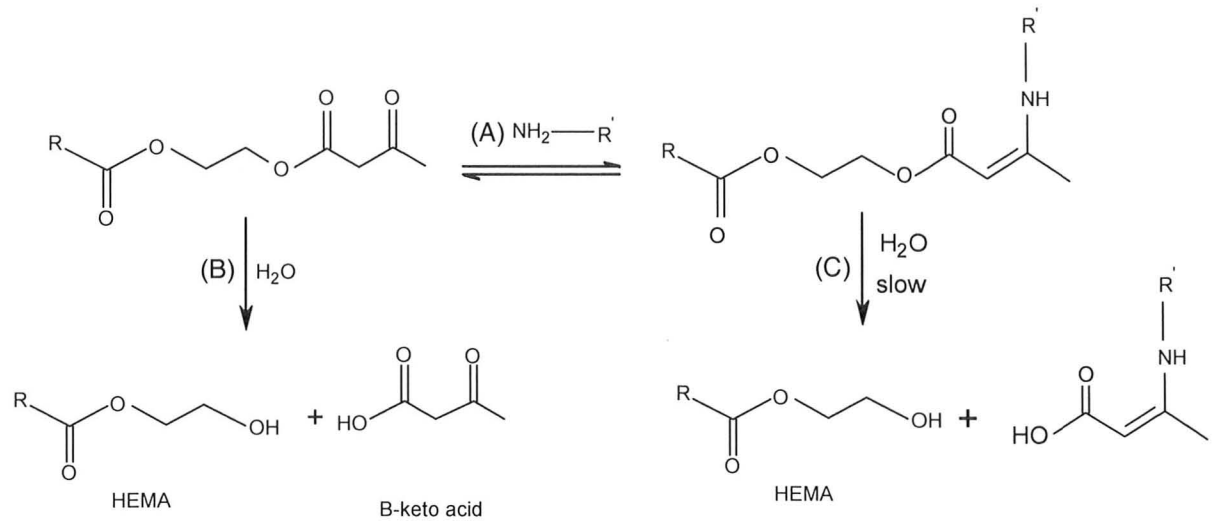

Scheme 2.2 **A.** Reversible enamine formation from acetoacetate and amine, **B.** Hydrolysis of acetoacetoxy ethoxy ester, **C.** Hydrolysis of ester group after enamine formation to release an a 3-amino-2-butenoic acid (or 3-aminocrotonic acid) fragment.

Our previous studies on coating calcium alginate capsules with self-crosslinking polyelectrolytes showed sequential deposition of A70 and PLL on calcium alginate capsules lead to a shell consisting of a covalently crosslinked polyelectrolyte complex.[91] These results led us to propose that the polydentate nature of the A70–PLL interactions helps maintain a higher level of enamine crosslinks than expected for small molecule analogs under comparable conditions. In other words, the high local concentration of reactive groups and their inability to diffuse apart when freed by the reversible reaction because of the electrostatic interactions, creates a mechanism to form a higher percentage of crosslink bonds, stabilizing the crosslinked network.

The present chapter describes two aspects of A70 chemistry that are relevant for such network formation. The first aspect involves the hydrolysis of the acetoacetate ester group of A70 upon copolymerization and dissolution in aqueous base, as well as during solution storage at 20° and 40°C, using ^{1}H-NMR. These studies allowed us to identify methods to dissolve this polymer in aqueous media with the least amount of hydrolysis, and further revealed the lifetime of the reactive polyanion in aqueous environments. The second aspect involves the rate and equilibrium position of the enamine formation between acetoacetate and amines, studied with the help of several small molecule, oligomeric and polymeric model systems. These include methyl acetoacetate (MAcAc) and 3-methoxypropylamine (MOPA) as small molecule models, polyanion (A70) and MOPA as a polymer-small molecule model, and polyanion (A70) and low molecular weight PLL, as a polymer-polymer model. These studies were carried out using UV/Vis spectroscopy and ^{1}H-NMR to determine the degrees of enamine formation under a variety of conditions in aqueous and organic environments.

2.3 Experimental

2.3.1 Materials

Methacrylic acid (MAA, 99%), 2-[methacryloyloxy] ethyl acetoacetate (MOEAA, 95%), poly-L-lysine hydrobromide (PLL, 1-5 kDa), 3-methoxypropylamine (MOPA), and methyl acetoacetate (MAcAc) were purchased from Sigma-Aldrich Co. 2,2'-Azobis(isobutyronitrile) (AIBN, 99.95%) from Dupont (Mississauga, ON) used as received. Diethyl ether, dimethyl sulfoxide (DMSO) and methanol (MeOH) were obtained from Caledon Laboratories Ltd. (Caledon, ON). Ethanol from Commercial Alcohols (Brampton, ON) was used as received. Hydrochloric acid solution was prepared from concentrates (FisherScientific) by diluting to 0.1 or 1 M with distilled water. Sodium hydroxide (NaOH) and sodium bicarbonate ($NaHCO_3$) were obtained from EMD Chemical Inc.

2.3.2 Synthesis of p (MAA-*co*-MOEAA) [70:30; A70]

Poly (methacrylic acid-*co*-2-[methacryloyloxy] ethyl acetoacetate) copolymer was prepared by free radical copolymerization. MAA (4.84 g, 56.2 mmol), MOEAA (5.16 g, 24.1 mmol) (mole ratio of MAA to MOEAA: 7/3) with AIBN (132 mg, 0.8 mmol, 1 mol% relative to total monomer) were dissolved in ethanol (100 mL) and reacted for 24 h at 60 °C. The polymer was isolated by precipitation in ethyl ether (2L) and then dried to a constant weight in a vacuum oven at 50 °C. Yield: 8.543 g (85.43 %).

2.3.3 Characterization of Polyanion (A70)

The composition of the p(MAA-*co*-MOEAA) was determined by ^{1}H nuclear magnetic resonance (^{1}H-NMR) spectroscopy using a Bruker AV 200 spectrometer for the polymer solution in DMSO-d6.

The molecular weight and molecular weight distribution (PDI) of A70 were estimated by gel permeation chromatography (GPC) with a system consisting of a Water 515 HPLC pump, Water 717 plus Autosampler, three columns (Waters Ultrahydrogel-120, -250, -500; 30 cm x 7.8 mm; 6μm particles) and a Water 2414 refractive index detector. The columns were adjusted at 35°C and narrow-dispersed PEG standards (Waters, Mississauga, ON) were utilized to calibrate the system. A 1% aqueous A70 solution at pH 7 was injected using a 20 microliter loop, and was eluted at a flow rate of 0.8 mL/min with an aqueous mobile phase that contained 300mM $NaNO_3$, 50mM phosphate and 20ppm NaN_3 at pH 7.

2.3.4 Study of A70 hydrolysis

The acid-form A70 (10 mg) obtained from the copolymerization was neutralized by adding a stoichiometric amount of 1 M NaOH (50 μL) relative to the methacrylic acid units, stirring until dissolution occurred, and then diluting to the desired polymer concentration, 1%, by addition of 940 μL D_2O. Also, another aqueous A70 solution was prepared by mixing the acid-form A70 (10 mg) with DMSO (30 mg) as plasticizer

(DMSO/A70: 3/1 w/w) for 20 min at room temperature, and then diluting and neutralizing the resulting mixture with stoichiometric amount of 0.05 M $NaHCO_3$ in D_2O.

The pH of both aqueous A70 solutions was adjusted to 7, and the resulting solutions were transferred to NMR tubes. The hydrolysis rate was determined at different temperatures by monitoring the ^{1}H-NMR spectra over time using a Bruker AV 200 spectrometer.

2.3.5 Study of enamine bond formation via the small molecule model

Methyl acetoacetate (MAcAc) solutions at 0.020, 0.040, 0.080, 0.16, and 0.64 M in DMSO, were mixed with equimolar amounts of a 10 w/w% solution of 3-methoxy propylamine (MOPA) in DMSO, at room temperature. For example, 16.2 μL (17.8 mg, 0.02mmol) of a 10 w/w% solution of MOPA in DMSO was added to 1.0 mL of a 0.020M solution of MAcAc in DMSO (equimolar AcAc/amine). Aliquots were taken at various times and diluted 1375-fold in MeOH to stop the reaction, and the amount of enamine was determined by UV/Vis spectroscopy.

The effect of acetic acid on the reaction rate in DMSO was determined. MAcAc solutions (0.020 M, 1.0 mL) in DMSO containing 0.51, 1.2 or 2.8 mg of acetic acid (mole ratio of MAcAc to acetic acid: 7/3, 1/1 and 3/7) were mixed with equimolar of a 10 w/w% of MOPA at room temperature and enamine formation was studied as explained above.

Enamine formation in aqueous environments was studied by following the equilibrium reaction between equimolar MAcAc and MOPA (0.02M) in distilled water at room temperature. Typically, 25.5 μL of an aqueous 7 w/w% solution of MOPA was added to 1 mL of a 0.02M aqueous solution of a MAcAc at room temperature. The pH of both reagent solutions was adjusted to physiological pH; the resulting reaction solution was at physiological pH as well. Aliquots of the reaction solution were diluted 1000-fold in distilled water and enamine content was measured by UV/Vis spectroscopy.

2.3.6 Study of enamine bond formation via the polymer-small molecule model

To study the enamine bond formation between A70 and MOPA in organic environment a 1% solution of acid-form A70 (0.02M acetoacetate) was prepared in DMSO, and reacted with equimolar MOPA. Typically, 20 μL (21.5mg 0.024 mmol) of a 10 w/w% solution of MOPA in DMSO was added to 1mL of a 1.0 w/w% solution of A70 (0.024 mmol acetoacetate) in DMSO at room temperature. The extent of enamine formation over time was determined by UV/Vis analysis, following dilution of the reaction solution in methanol.

The enamine bond formation in aqueous environment was determined by following the reaction between 1.0 w/w% A70 (neutral-form) and 7 w/w% MOPA in distilled water at the same concentration as in DMSO ([AcAc] = 0.02M) at physiological pH. Samples of the resulting aqueous reaction solution were removed at various times and then further diluted 1000-fold with distilled water prior to analysis by UV/Vis spectrophotometry.

2.3.7 Study of enamine bond hydrolysis in aqueous environment

The hydrolysis rate of enamine bonds were studied by diluting aliquots of an enamine solution in DMSO with various amounts of water. After various times in the aqueous solution, aliquots were removed, quenched by 1375-fold dilution in methanol and then analyzed by UV-Vis spectroscopy for enamine content. The initial enamine solutions were prepared by the reaction of acetoacetate and amine compounds in DMSO for 12 h at which point enamine formation was complete.

2.3.8 Study of enamine bond formation via the polymer-polymer model

The enamine bond formation via the polymer-polymer model was studied by the reaction between neutral-form A70 and PLL 1-5 kDa. For this purpose, 0.373 mL of an aqueous solution of 1.5 w/w% PLL (1-5k) was added to 1 mL of an aqueous solution of

1.25% w/w% A70 at physiological pH at room temperature (equimolar AcAc/amine, [AcAc]=0.0195M). The reaction solution was diluted 1000-fold in distilled water, and the enamine peak was monitored by UV/Vis spectrophotometer over 24 hours. The enamine bond stability at higher temperature was studied by subsequently heating the reaction solution at 37°C, followed by UV/Vis monitoring.

2.3.9 Spectrophotometric parameters of the enamine group

Using UV/Vis spectroscopy to determine the enamine content requires knowing the extinction coefficient of the enamine species involved. To measure the extinction coefficient of enamines formed from acetoacetate and amine, the reaction between MAcAc and MOPA, and also between A70 and MOPA, were studied by UV/Vis spectroscopy and ^{1}H-NMR. Typically, 20 μL (21.5mg 0.024 mmol) of a 10 w/w% solution of MOPA in DMSO was added to 1mL of a 1.0 w/w% solution of A70 (0.024 mmol acetoacetate) in DMSO at room temperature, and reacted overnight at room temperature. The enamine bond peak was measured by UV/Vis at ~290 nm following dilution in methanol.[92] Also, the conversion of a similar sample prepared in DMSO-d6 was measured by ^{1}H-NMR, and the extinction coefficient of enamine bond is measured by comparing the result of ^{1}H-NMR with UV/Vis spectrum.

The methanol dilution method of Nishihata et al (ref 95) was used to quench enamine formation/cleavage reactions for kinetic studies. The effect of methanol on enamine bond formation was studied for the reaction between A70 and MOPA by diluting the reaction solution a 1375-fold with methanol after 30 second reaction in DMSO and then checking the diluted solution by UV/Vis spectrometry immediately after dilution and after 1h. The UV absorption of pure DMSO, 1000-fold and 10,000-fold diluted DMSO in MeOH was measured at room temperature, as well.

The ability of methanol to arrest enamine hydrolysis in mixed organic/aqueous reactions was studied by diluting a reaction sample containing 90% water with methanol

after 30 second and 60 second hydrolysis, and the enamine concentration measured immediately and 30 min after dilution with methanol.

2.4 Result and Discussion

2.4.1 Characterization of p(MAA-*co*-MOEAA) [70:30; A70]

This work investigated the use of polyanions bearing reactive groups to react with PLL with formation of network supported by both ionic and covalent crosslinks. For this purpose a random copolymer of methacrylic acid (MAA) and 2-[methacryloyloxy] ethyl acetoacetate (MOEAA) at a mole ratio of MAA to MOEAA: 7/3 was prepared by AIBN initiated free radical polymerization in ethanol, and isolated by precipitation in diethyl ether. The chemical composition of the polyanion was determined from the ^{1}H-NMR spectrum measured in DMSO-d6. A comparison of the areas under the peaks at 4.1 and 4.3 ppm (CH_2CH_2 of MOEAA, "f" and "g" peaks) with the peak at 12.4 ppm (COOH of MAA) showed the polymer contains 70% MAA and 26% MOEAA; hence the polyanion was named A70 (Figure 2.1).

Also comparing the area under the peak at 4.8 ppm (OH of hydroxyethyl methacrylate, HEMA) with "f" and "g" peaks of MOEAA showed a trace of HEMA as a third component of the copolymer. HEMA has two other peaks at 3.5 and 3.9 ppm which overlap partially with "f" and "g" peaks of MOEAA (Figure 2.1).[97] The HEMA was likely formed by partial hydrolysis of MOEAA before, during or after polymerization. A70 was found to have a molecular weight (M_n) of 36 kDa and PDI of 2.8, by gel permeation chromatography (GPC).

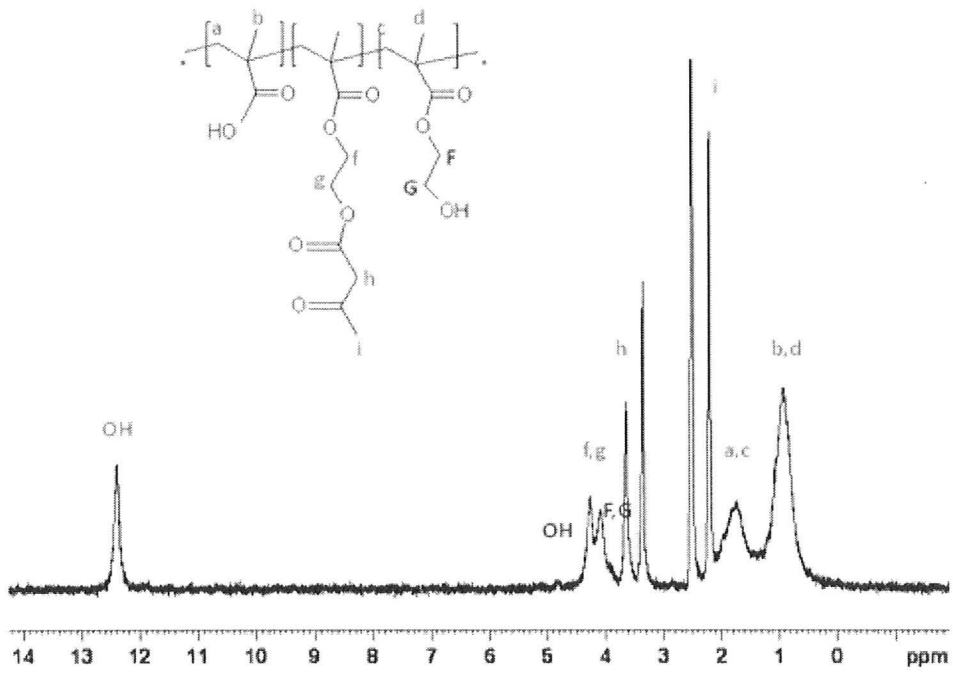

Figure 2.1 ^{1}H-NMR spectrum at 200 MHz of an A70 solution in DMSO-d6. Residual DMSO-d6 peak is at 2.5 ppm.

2.4.2 Study of A70 hydrolysis

Literature review noted that acetoacetate ester group of MOEAA-cotaining polymers can hydrolyze in aqueous media, especially at elevated temperature, to form hydroxyethyl methacrylate (HEMA) units and a β-keto acid, which would result in the loss of the reactive groups if it were to occur for A70.[92-94]

One challenge in using A70 is that the acid-form of A70 is insoluble in aqueous solutions required for reacting with PLL in the process of coating hydrogels. It was thus necessary to neutralize MAA groups to the point where the polymer was water soluble but under conditions where all or most of the acetoacetate ester groups survive dissolution. For this purpose, several different dissolution methods were examined. In the

first, a stoichiometric amount of 1M NaOH was added to the solid A70 (acid form) under stirring, and the resulting solution of A70-sodium form was then diluted with distilled water to the desired concentration. This procedure can expose the A70 to locally high concentrations of aqueous base. Figure 2.2 shows the ^{1}H-NMR spectrum of a 3% A70 solution prepared in this fashion in deuterium oxide. A comparison of the areas under the f and g peaks at 4.3 and 4.5 ppm (CH_2CH_2 of MOEAA) with the peaks at 3.9 and 4.1 ppm of HEMA showed that this dissolution method resulted in an A70 solution where 36% of the acetoacetate groups were hydrolyzed. The degree of hydrolysis does not increase much upon storage of this solution at 4°C indicating that much of the hydrolysis happens during the first minutes when the reaction mixture has a temporary excess of NaOH, together with undissolved A70.

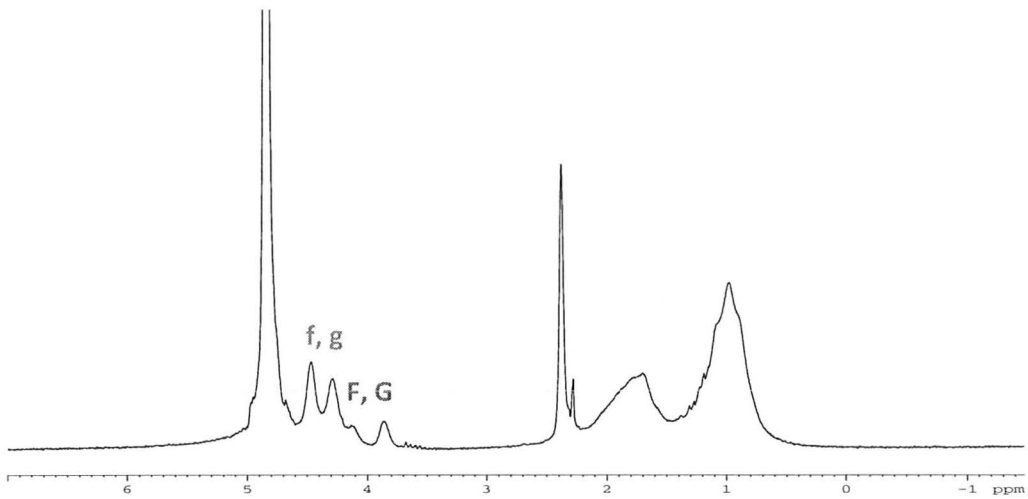

Figure 2.2 ^{1}H-NMR spectrum of A70 in D_2O prepared by addition of 1 eq of NaOH and D_2O to solid A70 (acid form).

According to these results it is necessary to develop a method to minimize the initial hydrolysis during dissolution of A70. This was done by searching for a water-miscible solvent that can dissolve the acid-form copolymer and allows it to be rapidly dispersed into aqueous base. The solvent should have low cytotoxicity as it will be

present in the aqueous solutions used for coating cell-containing alginate capsules. Also, availability in a deuterated version that would simplify ^{1}H-NMR analyses would be convenient. Finally, the base used was changed to dilute sodium bicarbonate solution, which has a much lower pH than the corresponding NaOH used previously.

Dimethyl sulfoxide (DMSO) was chosen for its good solvency properties and good cell compatibility.[98-100] The acid-form of A70 was mixed with DMSO as plasticizer (weight ratio of DMSO to A70: 3/1) for 20 min at room temperature, and then diluted with stoichiometric amount of 0.05 M $NaHCO_3$ in D_2O to give directly the desired final concentration. Under these conditions, the A70/DMSO mixture dissolved very fast (<5 min), and the pH observed after dissolution was 7.1.

The ^{1}H-NMR spectrum of the resulting A70 solution showed less initial hydrolysis (16%) occurred during dissolution (Figure 2.3). Similar results were observed when the dissolution was performed with 1 eq of NaOH rather than $NaHCO_3$. In all subsequent work, aqueous solutions of A70 were prepared by predissolving in DMSO.

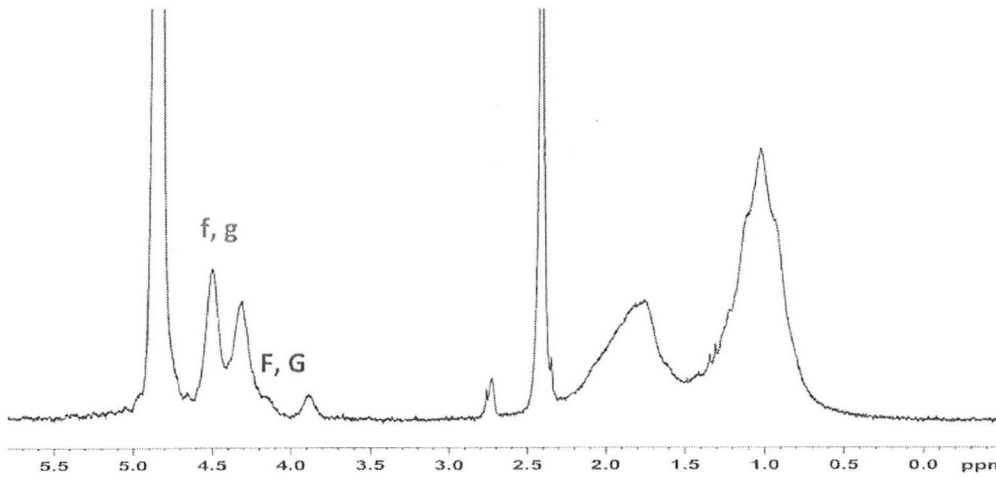

Figure 2.3 ^{1}H-NMR spectrum of A70 in D_2O prepared by plasticizing in DMSO and dissolving in 1 eq of 0.05M $NaHCO_3$.

The resulting solution was divided into two aliquots and stored for 32 days at both room temperature and 40°C, and the percent hydrolysis measured over this time (Fig. 2.4). Hydrolysis of the acetoaetate ester reached 41% after 32 days at room temperature, and 83% after 32 days at 40°C. This hydrolysis should affect the longevity of enamine-crosslinked networks, since enamine formation is reversible in aqueous environments. The combination of enamine reversibility to acetoacetate and acetoacetate ester hydrolysis thus provides a mechanism to reduce the acetoacetate concentration and thus decrease the possibility of reforming covalent crosslinks.

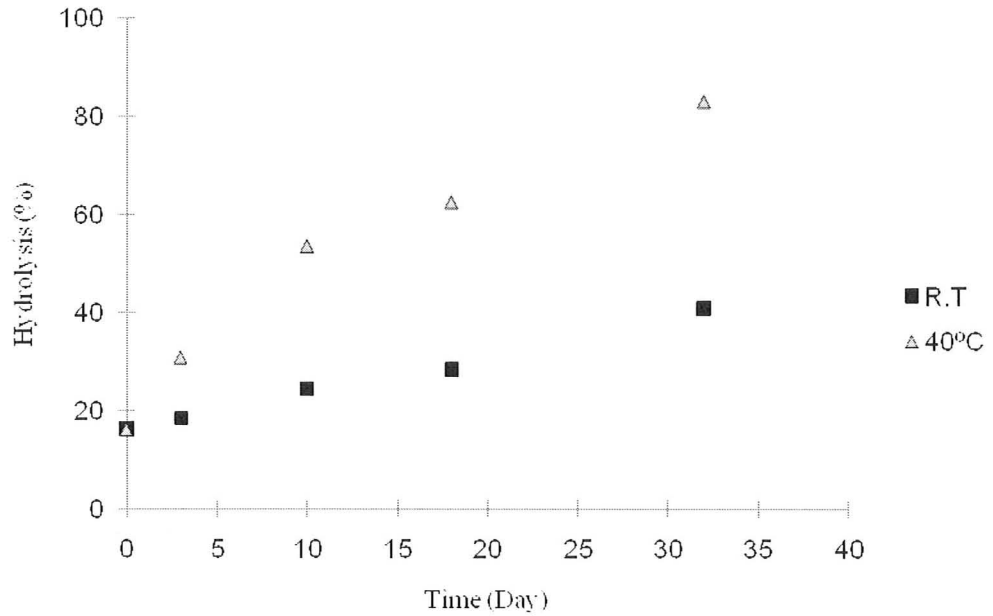

Figure 2.4 A70 hydrolysis at room temperature (R.T. = 20 °C) and 40°C for 3% A70 solutions at an initial pH of ~7.5.

2.4.3 Study of enamine bond formation and stability by UV/Vis

Literature review showed that the enamine formation between acetoacetate and amine proceeds at room temperature.[93] However, enamine formation is reversible depending on temperature, pH and reactant concentration. Thus it is necessary to study

the formation of enamine bonds between acetoacetate ester of A70 and amine, and study the stability of the resulting covalent bond in aqueous solution. It is difficult to study these reactions directly on the PLL/A70 system, due to the insoluble nature of the crosslinked network formed. Therefore, three different model systems were developed: 1) small molecule model, 2) polymer-small molecule model and 3) polymer-polymer model (involving low MW PLL). These model systems are more easily characterized by spectroscopic techniques and allow the effects of polymer structure and electrostatic interaction on enamine bond formation and stability in organic and aqueous environment to be examined.

The small molecules which are used in this study should resemble both PLL and A70 in terms of reactive group and solubility. Therefore, a primary amine, 3-methoxypropylamine (MOPA), and methyl acetoacetate (MAcAc) were chosen as mono-functional molecules with suitable solubility in either organic or aqueous environment. These molecules are free of any other functional group that could affect the enamine bond formation, and also cannot form any electrostatic network in aqueous or organic environments. To study the enamine formation in organic environment DMSO was chosen as the organic solvent because it is useful for NMR analysis and it is a good solvent for A70 allowing comparison between the small-molecule and polymer results. However, the UV/Vis spectrum of neat DMSO showed a broad peak extending to about 300nm which overlaps with the enamine absorption at ~290nm. Fortunately, the DMSO absorption following thousand-fold dilution with methanol (Figure.2.5) shifted to lower wavelength and does not overlap with enamine peak at ~ 290nm. Thus, DMSO did not interfere with the measurement of enamine concentrations in this work, which were determined after 1375-fold dilutions in methanol in most cases.

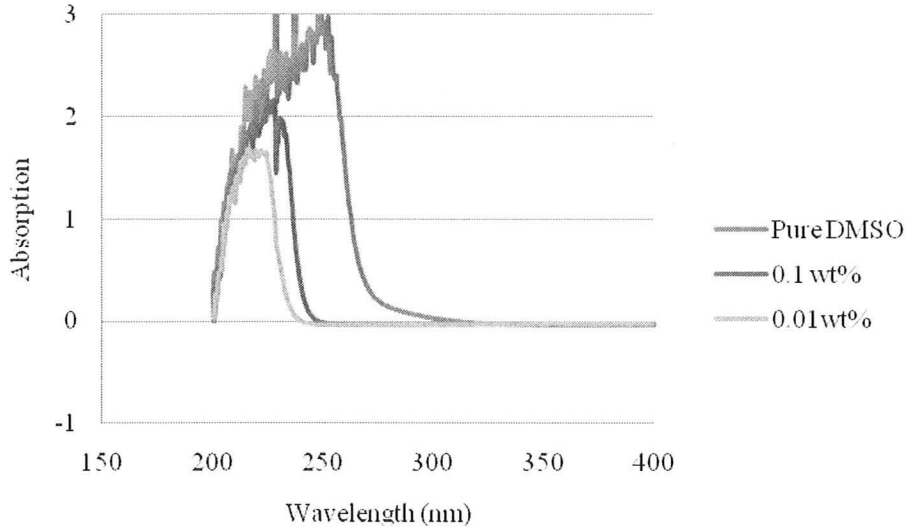

Figure 2.5 Absorption spectrum of DMSO in methanol.

To measure the extinction coefficient of the enamine group for the model systems, reactions between equimolar amounts of acetoacetate and amine compounds in DMSO were allowed to proceed to high conversion (typically about 100%) as determined by ^{1}H-NMR, and then an aliquot was diluted in methanol and analyzed by UV/Vis spectroscopy. For example, the ^{1}H- NMR spectrum of following reaction of A70 and MOPA in DMSO (24 mmol of each of the acetoacetate and amine groups) for 18h at room temperature is shown in Figure 2.6. The peaks due to the acetoacetate groups of A70 and the sharp peaks of the small-molecule amine have disappeared and been replaced with peaks due to the enamine. Enamines are typically formed as a mixture of *cis* and *trans* isomers which is evident in Figure 2.6 in the pairs of peaks labelled K, L and M. The enamine product consists of 60% *cis* (L at 8.5 ppm) and 40% *trans* (L at 6.7 ppm) which matches with the data Sanchez and Aldave report that described the *cis* structure as the most common product due to the hydrogen bonding between the oxygen of the carbonyl group and the hydrogen of the amine.[101] In their work, the percentage of *trans* product depended on solvent and varied from 5% in $CDCl_3$ to 42% in DMSO. The

conversion in DMSO-d6 overnight at room temperature was measured by ^{1}H-NMR to be about 100%, by comparing the integrations of the amide protons "L" and the methyl protons "d". Presence of two separate peaks for methylene protons "M" and methyl protons "K" confirms the presence of *cis* and *trans* enamine products as well.

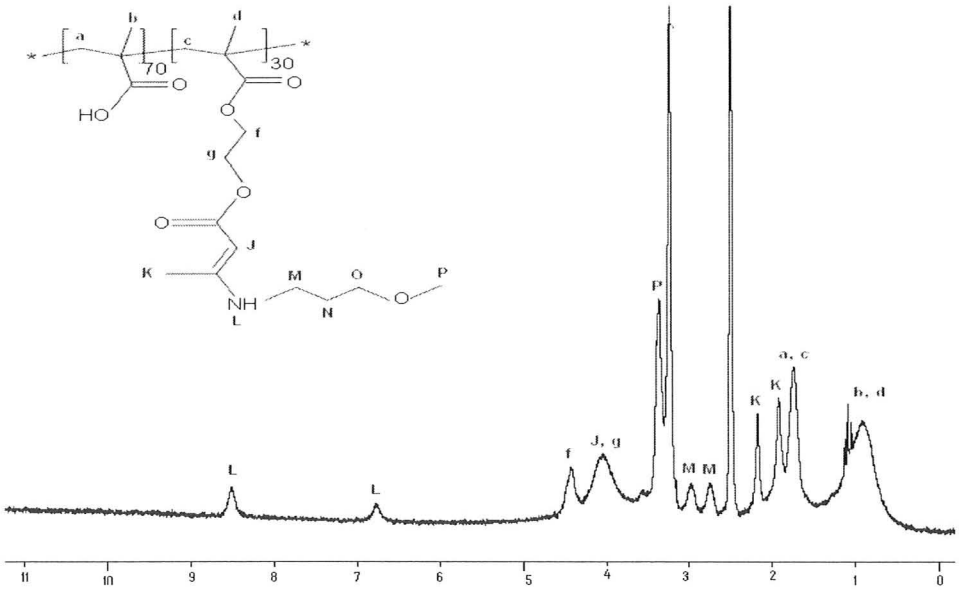

Figure 2.6 ^{1}H-NMR spectrum of the product of the overnight reaction between stoichiometric amounts of A70 and MOPA in DMSO-d6.

An aliquot of the reaction mixture was diluted 1375-fold with methanol and analyzed by UV/Vis (Figure 2.7). The measured UV/Vis absorption of 0.373 at 285 nm thus corresponds to an extinction coefficient of the enamine bond of **19,300** $M^{-1}cm^{-1}$. The extinction coefficient of the enamine formed by the reaction between MAcAc and MOPA in DMSO was measured in the same fashion, and showed a similar value (21,400 $M^{-1}cm^{-1}$).

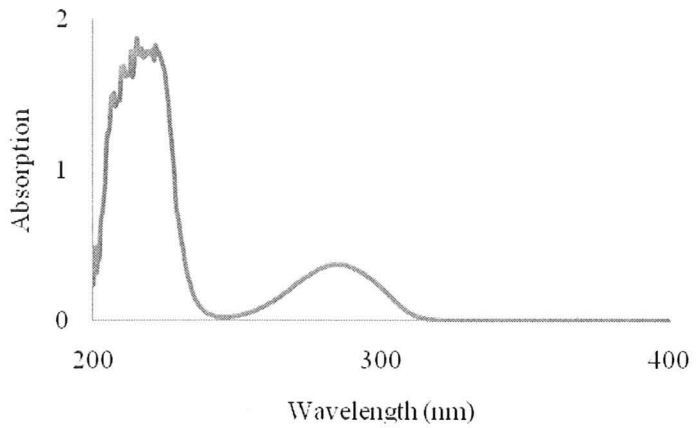

Figure 2.7 UV/Vis spectrum of the product of the overnight reaction between A70 and MOPA in DMSO after 1375-fold dilution with methanol.

Dilution with a large excess of methanol was suggested by Nishihata et al. in 1984 as a means of quenching enamine bond formation and hydrolysis during analogous aqueous experiments.[95] The effect of methanol on enamine bond formation was hence studied for our system by diluting the reaction solution 1375-fold with methanol after 30 second reaction in DMSO. UV/Vis analysis of the resulting solution showed 21.8% enamine bond. One hour after dilution with methanol, the enamine level was shown to be 22%, supporting Nishihata's suggestion that enamines are reasonably stable in methanol. Another aliquot of the reaction solution was diluted with methanol after 30 minutes reaction time in DMSO, showing 72% enamine formation.

The ability of methanol to also arrest enamine hydrolysis in mixed organic/aqueous reactions was confirmed by diluting an enamine sample (A70 + MOPA, DMSO, 80% conversion) with water so that it contained 90% water and then diluting it further with methanol after 30 second hydrolysis. UV/Vis analysis of this methanol-quenched sample, taken within 1 minute of dilution with methanol, showed 53.8% enamine, which dropped to 50.8% after another 30min in methanol. In contrast, dilution with methanol after 60 seconds hydrolysis showed 20.6% enamine bond, confirming that diluting in excess methanol indeed freezes the enamine content.

2.4.4 Study the enamine bond formation and stability via small molecule model, MAcAc-MOPA

The rate of enamine bond formation between MAcAc and MOPA in DMSO as a function of reagent concentrations was measured at room temperature over time by UV/Vis as described in part 2.2.5. Aliquots were removed from the DMSO reaction and diluted 1375-fold with methanol prior to UV/Vis measurements. Figure 2.8 shows that enamine formation is slow and likely incomplete at low reagent concentration, while it is essentially complete at 95% for 0.64M after 2 hrs.

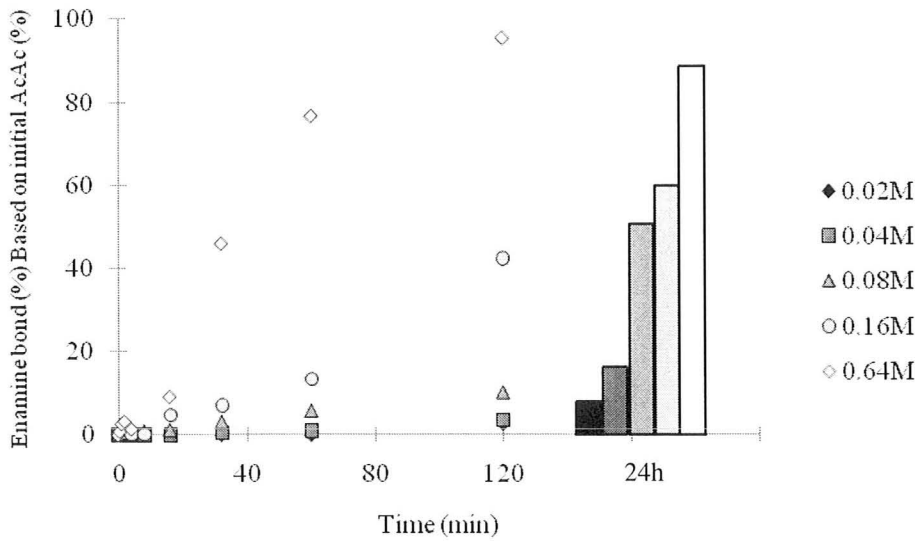

Figure 2.8 Enamine formation from MAcAc and MOPA in DMSO at room temperature (20°C), as function of reagent concentrations.

One interesting observation was that the reaction of A70 with MOPA appeared to be much more rapid, as described in the following section, perhaps due to the presence of 70 mol% methacrylic acid groups in the A70 structure. The effect of acid on the reactivity of acetoacetate was studied by dissolving acetic acid in 0.02 M MAcAc

solution in DMSO. In particular the mole ratio of MAcAc to acetic acid was chosen 3/7 to imitate the ratio present in A70, and the resulting solution was mixed with equimolar MOPA at room temperature. Also, solutions with mole ratios of MAcAc to acetic acid 1/1 and 7/3 were prepared to study the effect of acid concentration on the desired reaction.

The acid-containing mixture (mole ratio of MAcAc/acetic acid: 3/7) showed more rapid enamine formation with 53% formed after 2h reaction in comparison to only 2.5% without acetic acid (Figure 2.9). The reaction mixtures of lower acid content demonstrated a similar trend with slower velocities. Acetic acid has two opposite roles, it protonates methyl acetoacetate as well as MOPA. However, amine protonation decreases the reactivity of amine but the conjugate acid of the carbonyl group is a better electrophile than the neutral carbonyl group itself, and can accelerate the enamine bond formation rate. According to our results the catalyst role of acetic acid is much more effective than the inhibitor role in organic solvent and increases the enamine bond formation rate especially at lower mole ratio of MAcAc to acetic acid (Figure 2.10).

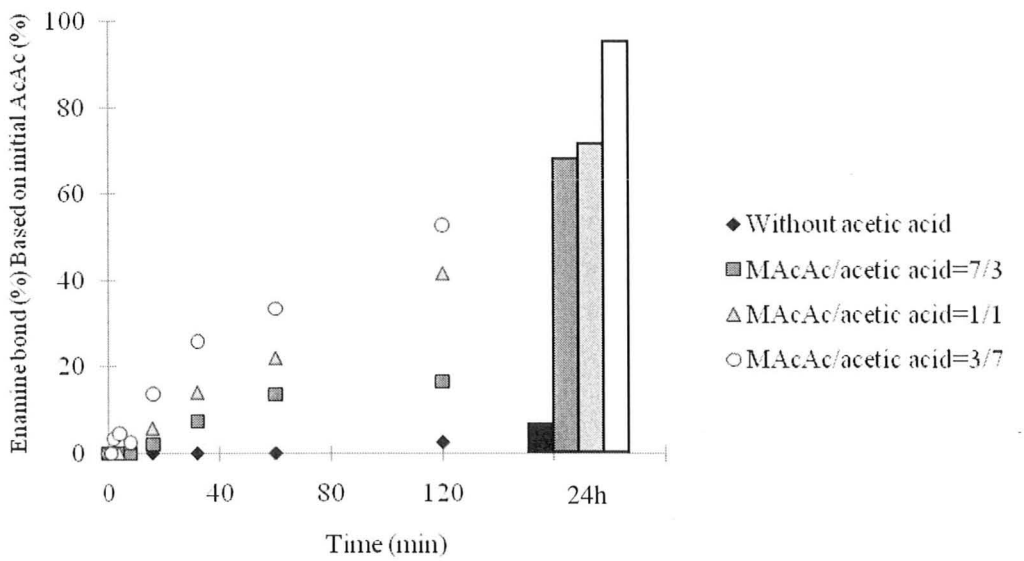

Figure 2.9 Enamine formation for the reaction at room temperature (20°C) between MAcAc and MOPA (20 mM each) in DMSO in the presence of acetic acid.

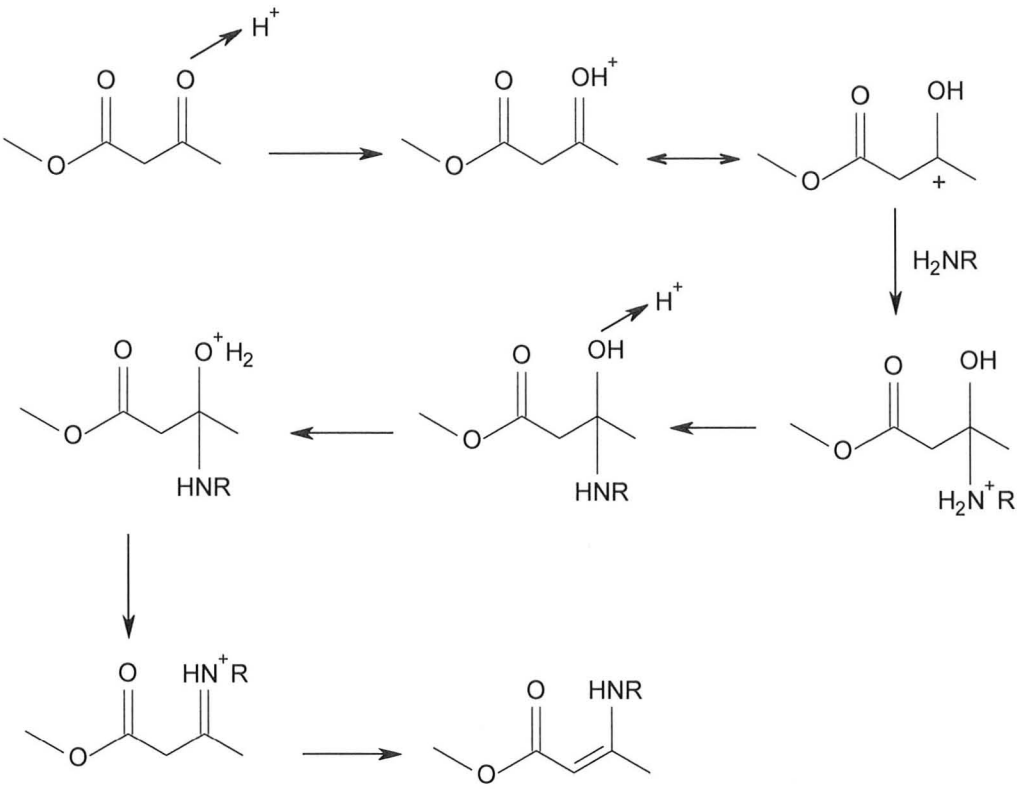

Figure 2.10 Mechanism of acid catalyzed reaction between MAcAc and MOPA.

The enamine sample formed in the presence of acetic acid (MAcAc/acetic acid: 3/7) was diluted with HEPES buffer at pH 7.8 (HEPES buffer: DMSO = 90:10 vol ratio) and then analyzed by UV/Vis spectroscopy for the occurrence of hydrolysis. Hydrolysis was rapid with about half the enamine consumed in a first 2h. When only 10% water was present, hydrolysis was much slower with little change in enamine content detected after 24h (Figure 2.11). Thus, it appears that the enamine is unstable and is hydrolyzed in solutions with significant water content.

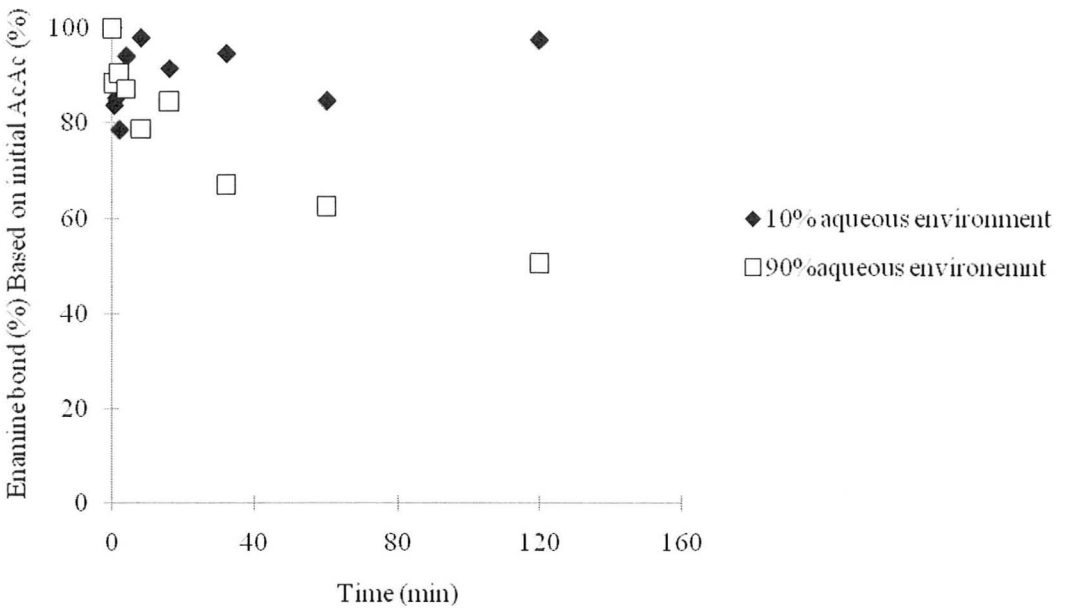

Figure 2.11 Enamine hydrolysis rate for the reaction between MAcAc and MOPA in DMSO at room temperature (20°C).

To further probe the stability of the enamine in aqueous solution, the reaction between MAcAc and MOPA ([AcAc] = [MOPA] = 0.02M) in distilled water at pH~7 was attempted. UV/Vis analysis showed no detectable enamine bond formation even after 24h at room temperature.

2.4.5 Study the enamine bond formation and stability via polymer-small molecule model, A70-MOPA

Enamine formation from A70 (acid form) and MOPA (equimolar AcAc /amine, [AcAc] = 0.02M) in DMSO approached 100% after 1h with an estimated half-life time of formation of 2 minutes (Figure 2.12). Comparing the A70-MOPA reaction in DMSO with the analogous small molecule model reaction showed faster reaction for A70 than MAcAc in organic environment. This is largely attributed to the acid catalysis provided by the methacrylic acid units in A70 (acid form). However, the A70-MOPA mixture

showed higher enamine bond formation after 2h reaction (92.8% vs. 53%) than the small molecule model containing acetic acid at the same concentration as the MAA units. According to these results we suggest that the higher enamine level in polymer-small molecule model is the effect of higher local concentration of acetoacetate and methacrylic acid in polymer structure (A70) in comparison to their concentration in the small molecule model.

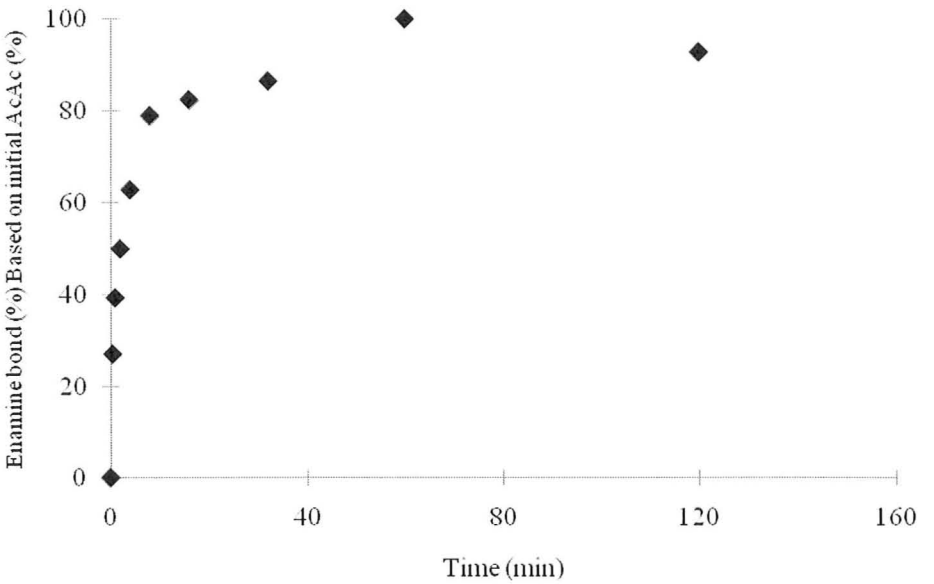

Figure 2.12 Enamine formation rate for the reaction between A70 and MOPA in DMSO at room temperature (20°C).

Hydrolysis of the polymer-small-molecule enamine (A70-MOPA) in solutions containing different amounts of HEPES buffer at pH 7.8 was examined and the results are shown in Figure 2.13. Enamine levels descend quicker as the water content is increased to the extent that 60% of all the enamine bonds are cleaved after 2h hydrolysis in 90% aqueous environment, conditions considered close to the pure aqueous conditions encountered by the hydrogels. According to these results, enamine bond forms rapidly in

DMSO, with a half-life time of formation of 2min, and decomposes quickly and permanently in aqueous conditions.

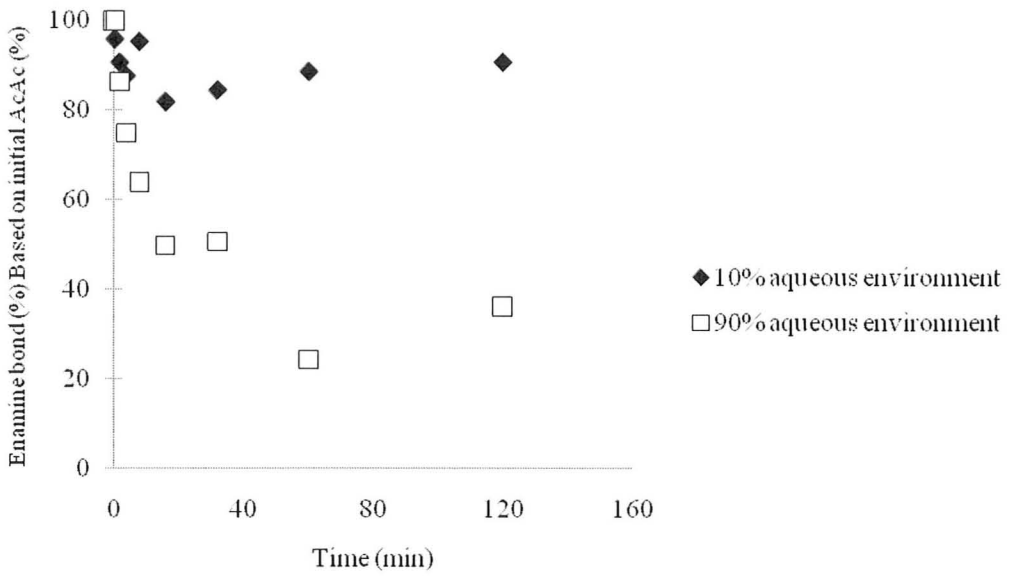

Figure 2.13 Hydrolysis of the enamine formed by reaction of A70 and MOPA in DMSO as a function of the water content at room temperature (20°C).

UV/Vis analysis of the reaction between A70 and MOPA in distilled water at the same concentrations as in DMSO ([AcAc] = 0.02M) at pH~7 showed low level enamine bond formation, reaching 0.8% after 30 seconds and plateauing at 1.1% after 2 h of reaction. In fact, enamine bond is not stable in aqueous environment and might cleave.

2.4.6 Study the enamine bond formation and stability via polymer-polymer model, A70-PLL

UV/Vis analysis of the reaction between A70 and PLL 1-5 kDa (equimolar AcAc/amine, [AcAc] = 0.02M) at physiological pH in distilled water as the more similar model to the real condition (microcapsule) showed higher enamine level (~12%) in

comparison to the small molecule and polymer-small molecule models (Figure 2.14). In this system, two explanations can be considered based on the polyelectrolyte complexation for the enhanced enamine bond formation compared to the systems where one or both reactants are small-molecules: one involves the high local concentration of reactants and the other is the creation of hydrophobic microenvironments. Previous studies showed that hydrophobic environment improves the rate of enamine bond formation.[102] In our system, polymer-polymer model, the electrostatic network formed between low MW PLL (polycation) and A70 (polyanion) provides a hydrophobic microenvironment that contains more polymer and less water than the initial reaction solution as well as a high local concentration of the reactants. Our results of the small molecule model and polymer-small molecule model showed enamine bond forms quickly in hydrophobic environment (DMSO), and the reaction rate depends on reactant concentration and acid catalyst. Thus we suggest that the hydrophobic microenvironment and higher concentration of reactants for the PLL-A70 system helps maintain higher levels of enamine bonds than expected for small molecule model and polymer-small molecule model analogs under comparable condition.

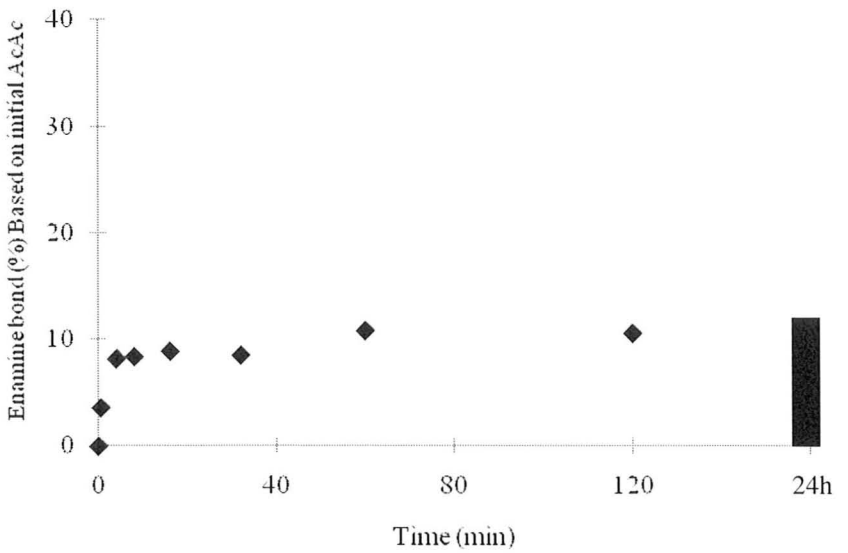

Figure 2.14 Enamine formation rate for the reaction between A70 and PLL in aqueous environment.

UV/Vis analysis of the polymer-polymer model while storing at 37°C showed that the enamine bond level decreases over time, 2.9% after 20 days (Figure 2.15). Regarding the hydrolysis rate of enamine bond in small molecule model and polymer-small molecule model, enamine bond is reversible and has short life time in aqueous environment. In polymer-polymer model the hydrolyzed enamine bond can reform in the hydrophobic microenvironment in the presence of acetoacetate group. However, the continuous hydrolysis of acetoacetate at elevated temperature (37°C) provides less acetoacetate groups to form enamine bond, thus enamine content of the network decreases slowly but permanently.

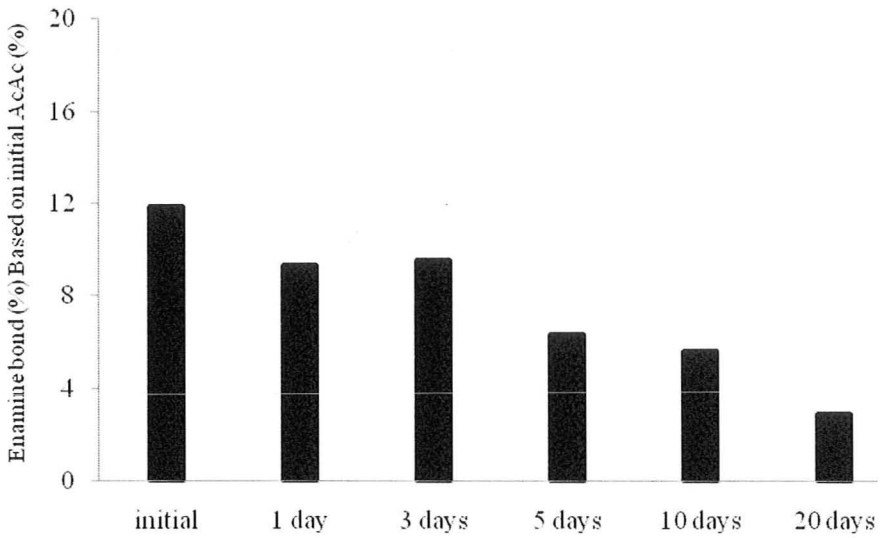

Figure 2.15 Hydrolysis of the enamine formed by reaction of A70 and PLL in aqueous environment at 37°C.

2.5 Conclusion

This report describes an improved method for dissolving A70 that largely avoids temporary excursions to high pH, and thus limits the initial hydrolysis. However,

hydrolysis continues over time at neutral pH, leading to near complete hydrolysis after 32 days at 40°C.

The enamine bond formation was studied in organic and aqueous environment via different molecular models. This study showed low level enamine bond for the small molecule and polymer-small molecule model in aqueous environment. The enamine bond level improves in polymer-polymer model in aqueous environment due to higher local concentration of reagents and the hydrophobic environment formed by the electrostatic interaction between PLL and A70. However the covalent bonds slowly but permanently cleave at physiological pH. This means that the combination of enamine reversibility and acetoacetate hydrolysis creates a mechanism for slowly but permanently removing covalent crosslinks even from an initially quite strong A70-PLL network. In turn, this implies that these networks, in contrast to those formed using more permanent amide-based crosslinks, should be considered to be temporary networks with a significant potential for applications that require protection of cells just for the time needed to develop their own extracellular matrix, and as such can certainly find valuable uses in the field of cell encapsulation.

Chapter 3: Core Crosslinked Alginate Microcapsule

3.1 Abstract

Self-crosslinkable polyelectrolytes were used to prepare core-crosslinked CaAlg capsules. In this study the polyanion poly(methacrylic acid-*co*-2-[methacryloyloxy] ethyl acetoacetate) (70:30 mole ratio, A70), as well as its fluorescently labeled analog (A70f), are added to alginate solution, and dropped into a calcium chloride gelling bath. The resulting calcium alginate capsules displayed a homogenous distribution of A70f throughout the core. Exposure of these capsules to different molecular weights of rhodamine-labelled PLL resulted in deep penetration of low MW PLLr (4-15 kDa), while higher MW PLLr (15-30 kDa) was mainly captured in the shell as revealed by CLSM. In the later case, A70f was seen to diffuse to the surface of the capsules. Challenging the capsules with 70mM sodium citrate and 0.1M sodium hydroxide showed absence of covalent crosslinking in the bead core. This lack of core-crosslinking is attributed to A70 migration to the shell, possibly preventing higher MW PLL diffusion to the core, thus resulting in shell-crosslinked capsules. These crosslinked shells, while stable for extended periods of time at room temperature, were found to degrade under physiological conditions within weeks, in agreement with model experiments. These networks may thus be suitable for temporary protection of encapsulated cells for the time needed to develop their own extracellular matrix.

3.2 Introduction

The inability or loss of the ability of the body to produce essential enzymes or hormones is the cause of many diseases such as Parkinsons, Alzheimers, diabetes, liver failure, hemophilia etc. Cell microencapsulation is a known concept of transferring cells to treat such pathological conditions. Cell encapsulation involves forming a selectively permeable membrane containing therapeutic cells, that allows in-diffusion of nutrients, oxygen, and growth factors for cell metabolism, as well as out-diffusion of waste products and therapeutic proteins. Moreover, cells and larger molecules of the immune system are kept out, avoiding the need for cytotoxic immunosuppressant drugs. [4, 5] Different parameters such as biocompatibility, permeability, and chemical-mechanical stability should be considered when designing a microcapsule structure. One of the most frequently employed microcapsules is the alginate/PLL/alginate capsule (APA). Alginate, the most common ionotropic cell embedding material, is a negatively-charged, linear polysaccharide (PS). Specifically, it is a copolymer of 1, 4-linked β-D- mannuronic acid (M) and α-L-guluronic acid (G). The G-rich region of alginate forms a three dimensional interconnected network at room temperature or any other temperature up to 100°C in the presence of divalent cations such as calcium.[38-40] In alginate hydrogels the M/G ratio,[47-50] alginate MW,[51] and type of divalent ion[42, 52-54] can affect properties such as gel permeability, gel strength and biocompatibility. APA capsules are formed by polyelectrolyte complexation between alginate (polyanion), and PLL (polycation) around a calcium alginate gel core. In this approach the calcium alginate capsules are first coated with PLL solution followed by exposure to sodium alginate in a layer-by-layer process (LBL), designed to increase the hydrogel stability and optimize its permeability.[61] In this structure, PLL interacts with negative charges on and near the surface of alginate capsules[11]. While some previous studies reported successful long-term implantation of microencapsulated allografts in APA capsules for spontaneously diabetic dogs and humans, [65, 66] clinical applications are still far off due to PLL protein absorption.[67-70] Studying the surface chemical composition of APA capsules revealed that calcium alginate core is covered by a single layer membrane wherein alginate and PLL are

interacting to form PEC complex. In fact, PLL is uniformly distributed among the capsule surface, and a distinct outer layer of alginate does not exist.[70] This PEC complex weakens over time, exposing more immunogenic PLL chains to the host.[50, 74] As well, alginate, depending on the source and processing, contains variable amounts of impurities such as endotoxins, proteins and polyphenols that can be reduced but not completely removed during purification.[72, 73, 75-77]

Several synthetic polymers have been investigated as potential replacements of alginate and/or PLL with the goal of producing capsules with improved biocompatibility and increased chemical/mechanical stability. In this area some synthetic polymers such as poly(hydroxyethyl methacrylate-co-methyl methacrylate), [103] and the product of Michael addition between thiol and acrylate end-functionalized pluronics polymers[86] have been used to form capsules entirely composed of synthetic polymers, with the second example involving a covalently crosslinked network. Also, reactive polyelectrolytes such as α-phenoxycinnamylidene-acetylated poly(allylamine),[87] have been used to form a photo-crosslinked shell around a calcium alginate core.

Another approach to strengthening the capsules is to form a crosslinked network inside the alginate core. Several studies produced functionalized alginate by the chemical introduction of reactive groups such as thiol,[79-81] methacrylate and acrylate[82-85] on the alginate backbone. The functionalized alginate capsules are crosslinked by exposure to a second polymer, catalyst or light; however, applications are limited by the interference of the functional group in alginate gelation. In fact, the lack of selectivity during chemical modification that generally occurs on both guluronic acid (G) and mannuronic acid (M) interferes with the instantaneous alginate gelation in the gelling bath, and hence affects its application for cell encapsulation.[84, 85] To form a crosslinked network inside the alginate capsule without negative effect on gel formation properties, a possible approach can be the development of interpenetrating polymer systems (IPN) or semi-interpenetrating polymer systems (semi-IPN). The resulting composite hydrogel forms a new structure with completely different properties in comparison to the initial materials. Such studies were done on composites of alginate with methacrylated derivatives of dextran,[104]

chitosan,[105] cationic methacrylate monomer,[106] silica,[107] and acrylate-N-vinylpyrrolidone [108] to improve mechanical properties and biocompatibility of alginate capsules, with the least undesired effect on alginate gel properties.

Recently, we developed synthetic polyanions containing acetoacetate group, poly(methacrylic acid -*co*-2-[methacryloyloxy] ethyl acetoacetate) (70:30 mol%, A70), to form a tough crosslinked shell around PLL-coated calcium alginate capsules (CaAlg), and to reinforce the CaAlg core by forming covalent bonds with PLL and other polyamines. [89-91] This approach is based on electrostatic attraction and preconcentration of the reactive polyelectrolytes with subsequent covalent crosslinking in the absence of light, catalyst or initiator (Scheme 3.1).

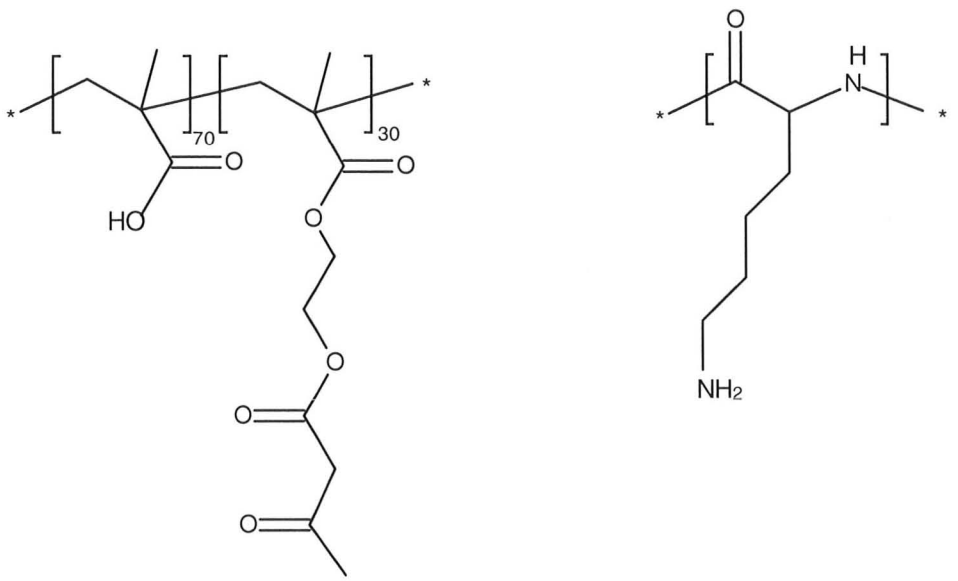

p(MAA-co-MOEAA) [70:30; A70] poly (L-Lysine), PLL

Scheme 3.1 Polyelectrolytes used in this study to reinforce CaAlg capsule.

In this study core-crosslinked CaAlg capsule were formed by mixing the polyanion (A70) with alginate solution, and CaAlg capsules containing A70 were formed in gelling bath. These capsules were then exposed to PLL designed to diffuse into the

CaAlg/A70 capsules and form covalent bonds with the A70. This was followed by a final A70 coating to crosslink and neutralize surface-complexed PLL. Forming such covalently crosslinked CaAlg cores depends on the distribution and mobility of A70 in alginate gel, PLL diffusion, polyelectrolyte MW and enamine bond formation rate. Therefore, two scenarios were studied depending on the relative ability of reactive polyelectrolytes to diffuse through the alginate capsule matrix (Scheme 3.2):

1. Larger PLL chains (higher PLL MW) should be restricted to the capsule surface, and covalently crosslink with A70 chains to form a shell. If the A70 in the CaAlg core is mobile it may diffuse to the capsule surface to react with the PLL bound there. The thickness of the resulting shell should reflect the relative diffusion rate of polyelectrolytes.
2. Smaller PLL chains (lower PLL MW) should penetrate into the CaAlg capsule and form PEC complexes and covalent bonds in the bead interior. However, these PLL chains should still be long enough to effectively crosslink the A70 into an extended network.

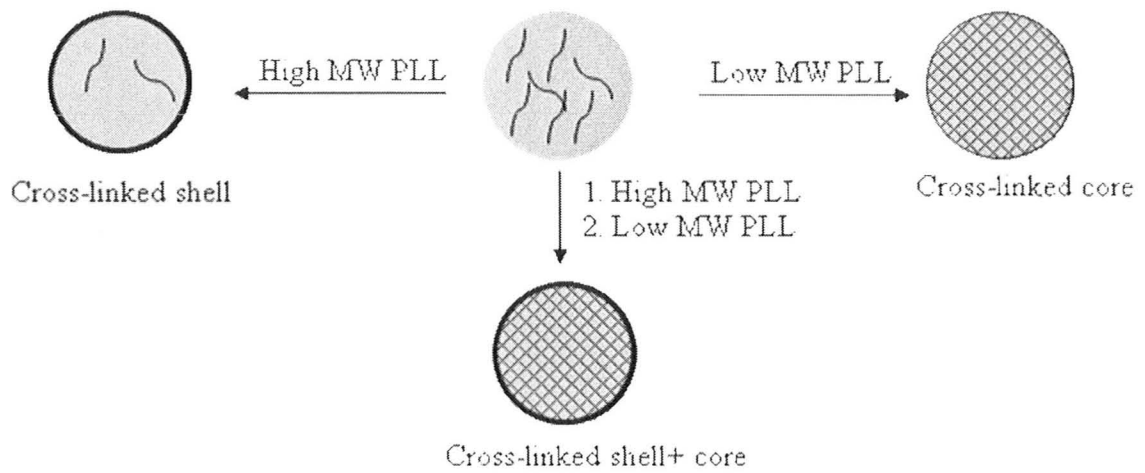

Scheme 3.2 Capsule morphology depending on MW of PLL when embedding the reactive polyanion within the CaAlg capsule.[91]

In both scenarios the diffusion ability of polyelectrolytes depends on alginate gel pore size, polyelectrolyte MW, and the polyelectrolyte interaction with alginate and calcium ion. In previous research in our group, J. Mazumder had made core-crosslinked CaAlg capsules by mixing A70 of molecular weight of 42kDa with low G content alginate formulation (Kelton LVCR, M/G: 1.5 (40% G)[89]). This study showed that high MW PLL (15-30 kDa) was restricted to the outer surface where a crosslinked shell forms. On the other hand, low MW PLL (1-4 kDa) showed homogenous distribution within the capsules, but was too short to effectively crosslink the A70 chains. Medium MW PLL (4-15 kDa) represented a promising compromise between ease of in-diffusion and ability to crosslink. The capsules formed by PLL 4-15 kDa retained their core-crosslinked appearance even after manual cutting and treatment with citrate, 2M NaCl and 0.1M NaOH, demonstrating that sufficient PLL has diffused into the core and crosslinked with A70. These capsules also showed good cell viability for C_2C_{12} cells which indicates suitable permeability of nutrients into the capsules. Fluorescently labelled dextrans were used to determine that these capsules had molecular weight cut-off around 100-200kDa.[91] In this chapter, the interaction of polyelectrolytes with new alginate at higher G content and viscosity (Pronova UP MVG, G/M: 1.5 (≥60% G))[109] as a more commonly used alginate in pharmaceutical application, PLL diffusion, A70 mobility, and the chemical stability of crosslinked bond under physiological condition were studied. In this study CLSM, UV-Vis analysis and optical microscopy were applied to characterize polyelectrolyte absorption and distribution. Also CaAlg composite capsules were exposed to 70mM citrate and 0.1M NaOH to study the enamine bond formation and its stability at physiological condition.

3.3 Experimental

3.3.1 Materials

Sodium alginate (Pronova UP MVG) was purchased from NovaMatrix. Methacrylic acid (MAA, 99%), 2-[methacryloyloxy] ethyl acetoacetate (MOEAA, 95%),

poly-L-lysine hydrobromide (PLL, Mn 4-15 kDa, 15-30 kDa and 40-60 kDa), fluorescein isothiocyanate (FITC, 90%), and triethylamine were purchased from Sigma-Aldrich Co. N-(3-aminopropyl) methacrylamide hydrochloride (APM) from Baker, and 2, 2'-azobis(isobutyronitrile) (AIBN, 99.95%) from Dupont (Mississauga, ON) were used as received. Sodium chloride (reagent), anhydrous diethyl ether, N, N-dimethylformamide (DMF), and dimethyl sulfoxide (DMSO) were obtained from Caledon Laboratories Ltd (Caledon, ON). Calcium chloride from Fisher, and ethanol from Commercial Alcohols was used as received. Hydrochloric acid solutions were prepared from concentrates (Fisher Scientific) by diluting to 0.1 or 1 M with distilled water. Sodium hydroxide (NaOH) and sodium bicarbonate ($NaHCO_3$) were obtained from EMD Chemical Inc.

3.3.2 Synthesis of p(MAA-*co*-MOEAA) [70:30; A70]

Poly(methacrylic acid-*co*-2-[methacryloyloxy]ethylacetoacetate) copolymer was prepared by free radical polymerization. For this purpose, MAA (4.84 g, 56.2 mmol), MOEAA (5.16 g, 24.1 mmol) (mole ratio of MAA to MOEAA: 7/3) and AIBN (132 mg, 0.8 mmol, 1 mol% relative to monomer) (mole ratio of monomers to initiator: 100/1) were dissolved in ethanol (100 mL) and reacted for 24 h at 60 °C. The polymer was isolated by precipitation in ethyl ether (2L) and then dried to a constant weight in a vacuum oven at 50 °C. Yield: 8.543 g (85.43 %), pK_a=7.1.[89]

3.3.3 Synthesis of fluorescently labelled A70, A70*f*

A70*f* was prepared with two different methods, labelling a pre-formed polymer or incorporation of a fluorophore during polymerization, as described below:

1. Labeling A70 by post-functionalization in aqueous solution, $A70f_{aq}$:

A70 (1 g, 2.41 mmol) was dissolved in 100 mL of water. The pH was adjusted to 9 by adding 0.1 M NaOH. FITC (93.8 mg, 0.241 mmol) dissolved in 2 mL of DMF was added to the polymer solution under stirring. The mixture was stirred for 24 h at room temperature. The FITC-labeled copolymer, A70f, was dialysed against deionized water using cellulose membranes (12-14 kg/mol MW cutoff, Spectrum Laboratories) for at least

5 days with daily water changes. The resulting polymer solution was freeze-dried. In this method, FITC was attached to the methylene group of acetoacetate in MOEAA.

2. Labeling A70 via copolymerization with a fluorescent monomer, A70*f*$_{org}$ (prepared and characterized by Dr. Nick Burke):

In this approach, A70*f* was prepared by copolymerization of MAA and MOEAA with a small amount of a fluorescent monomer, APM*f*, prepared by reaction of N-(3-aminopropyl) methacrylamide hydrochloride (APM) with FITC. The preparation of APM*f* and A70*f*$_{org}$ were done by Dr. Nick Burke and are described here briefly. APM (100mg, 0.56mmol) and FITC (218.5mg, 0.56mmol) were dissolved in DMF before adding triethylamine (62 mg, 0.61 mmol, 1.1 eq). The mixture was stirred for 3 days at room temperature. The FITC-labeled APM was precipitated in, and washed with, acidified water, and then vacuum dried at 20°C (yield: 86%). The FITC-labeled APM was copolymerized with MAA and MOEAA (feed ratio: 70/30/0.5; MAA/MOEAA/FITC-APM) in the presence of 1 mol% AIBN in ethanol for 20h at 65°C. The polymer was isolated by precipitation in ethyl ether and vacuum dried at 50-60°C. Yield: 89% and MW (M_n): 23kDa.

A100*f*, a non-reactive analog of A70*f*$_{org}$, was prepared in a similar fashion by Jared Wiseman and Nick Burke by copolymerization of MAA with 0.5 mol% APM*f*.

3.3.4 Synthesis of rhodamine-labelled poly (L-Lysine), PLLr

PLL with MW of 4-15 kDa, and 15-30 kDa (100 mg, 0.478 mmol of lysine·HBr units) were dissolved in 10 mL of 0.2 M $NaHCO_3$ buffer solution at pH 9 in a 20 mL glass vial. Rhodamine B isothiocyanate (RITC) (1.28 mg, 0.0239 mmol) dissolved in 0.5 mL of DMF was added to the PLL solution and the mixture was stirred for 1 h at 20 °C. The resulting solution was dialyzed for at least 5 days against deionized water using cellulose tubing (Spectrum Laboratories, 3.5 kDa MW cutoff) with daily water changes. The dialyzed polymer solutions were freeze-dried, and the polymers were dried further to constant weight in a vacuum oven at 50 °C.

3.3.5 Characterization of labelled polyanion, A70*f*

Dilute solutions of A70f (0.02%, $1.48x10^{-3}$ mM repeat units) was prepared in HEPES buffer at pH 7.8 and studied by UV-Vis spectroscopy at 490-495 nm to determine the fluorescein concentration. The labelling degree and efficiency were determined by comparing the label concentration with the polymer repeat unit concentration. The fluorescent emission intensity of A70*f* solutions was measured with a SPEX Fluorolog 3-22 fluorometer.

The loss of label from A70*f* in aqueous environment was studied by GPC and UV-Vis spectroscopy. In this method, 1% solutions of A70f in GPC aqueous mobile phase (300mM $NaNO_3$, 50mM phosphate and 20ppm NaN_3 at pH 7) was prepared and analyzed by GPC. The polymeric (>1500 g/mol) and low molecular weight (<1000 g/mol) fractions were collected separately; the amount of fluorescent material was measured by UV-Vis and compared with the initial amount of fluorescent material in the original 1% solution. A70*f* also was studied by ^{1}H-NMR and fluorescence microscopy to determine the effect of the labelling process on A70 hydrolysis and aggregation, respectively.

3.3.6 Characterization of labelled polycation, PLLr

Dilute solutions of PLLr (0.01%, $5x10^{-4}$ mM) were prepared in HEPES buffer and studied by UV-Vis spectrophotometer at ~ 557nm to define the labelling material concentration (RITC). The labelling efficiency and labelling degree were measured the same as in part 3.2.5.

3.3.7 Preparation of composite capsule, Ca (Alg/A70) capsule

The Ca (Alg/A70) capsules were prepared from a solution containing 1 or 1.5 wt% sodium alginate and 0.5 wt % A70 or A70*f*. The pH was adjusted to 7.5 with 0.1 M NaOH. The solutions were filtered with sterile filters (0.2 μm, Acrodisc Syringe Filter, Pall Corporation, U.S.A.). A syringe pump (Rassel Mechanical Inc. pump, model #A-99) was used to extrude this solution through a 27-gauge blunt needle (Popper & Sons, New

York) at a rate of 30.1 mL/h. A concentric airflow (3.75 L/min) passing by the needle tip is used to induce droplet formation. The droplets were collected in 60 mL of a 1.1 wt % calcium chloride and 0.45 wt % sodium chloride cold gelling bath. 10 min after capsule formation was completed, the supernatant was removed, and the resulting concentrated Ca (Alg/A70) composite capsule suspension (about 3 mL) was immersed in 10mL of new gelling bath solution for 10 min in the ice bath with occasional swirling. The supernatant was removed and the dense suspension of capsules (3 mL) was then exposed to 10mL of the desired concentration of PLL solution (4-15kDa or 15-30kDa) (pH~7.5) for 6 min in the ice bath with occasional swirling, and then washed with pre-cooled gelling bath and pre-cooled saline for 2 min. To coat capsules with A70, A70 solution (0.1%, pH~7.5) was added to the dense suspension of capsules (capsule/coating solution: 3/10), and let sit for 4 min with occasional swirling.

Final coated capsules were washed by immersing in saline for 2 min with occasional swirling, and stored at 4°C in saline for further use.

3.3.8 Composite capsule characterization

Capsules were examined with an Olympus BX-51 optical microscope fitted with a Q-Imaging Retiga EXi digital camera and ImagePro software. The average diameters of the capsules were determined by analyzing one batch of approximately 25-30 beads. Confocal images were taken with a ZEISS LSM 510 confocal laser scanning microscope (CLSM), fitted with air-cooled Argon and HeNe lasers (LASOS; LGK 7628-1) and running LSM 5 at detector gain 450 and 600 for A70f and PLLr, respectively. The Wild M40 optical microscope was used for phase contrast microscope images. The amount of polyelectrolyte absorption was studied by UV-Vis analysis of supernatant at different steps of forming capsules.

3.3.9 Chemical study of crosslinked network inside the composite capsule

Capsules were exposed to 70mM citrate for 30 minutes to extract calcium ions and leave only the polyelectrolyte complex network (electrostatic and covalent

interactions) to maintain the capsules. The resulting capsules were stored at 37°C in saline, and the diameter of microcapsules measured over time. The effect of storing at physiological temperature in aqueous solution on the degree of covalent (enamine) crosslinking was studied by exposing samples taken after different times of incubation to 0.1M NaOH (pH~13).

3.3.10 Study of A70 mobility inside the CaAlg composite capsule

The A70 movement in CaAlg (1.5%)/ A70f (0.5%) composite capsules was studied by optical microscopy. In this method capsules were placed on a microscope slide, covered by a glass cover slip, and examined by the fluorescence microscopy at room temperature. The cover slip seals the top and bottom surfaces of the capsules, transforming them into rounded cylinders that permit observation of out-diffusion of the A70*f*. Images were taken every 30 sec and the fluorescence intensity from representative areas in the centre of the capsule was measured using the ImagePro software.[110] The effect of exposure to polycation on A70 mobility in composite capsule core was determined by injecting two drops of 0.5% PLL 15-30kDa under the glass cover slip, and measuring the ratio of the fluorescence intensity at the capsules' centre to the continuous phase. As a control, these experiments were repeated with capsules containing A100*f*, an analog of A70*f* that is unable to form covalent bonds.

The effect of microscopy light on fluorescence bleaching was also defined. For this purpose capsules were covered with a glass cover slip, and exposed to continuous and non-continuous microscopy light with images taken every 30 sec. For non-continuous light the shutter was open for 3 sec before each image.

3.4 Result and Discussion

The purpose of this study is forming CaAlg composite capsules with a crosslinked interpenetrated network inside CaAlg core by the reaction between polyanion present in the core and the in-diffusing PLL. We had discussed in chapter 2 the chemistry of A70 and enamine bond formation and cleavage. According to these results A70

hydrolyzes over time at physiological condition (aqueous solution at 37°C, pH~7). Enamine bonds form spontaneously within the PEC complex formed by the electrostatic interaction between A70 and PLL. However, the covalent bonds slowly but permanently cleave at physiological condition. This means that the combination of enamine reversibility and acetoacetate hydrolysis creates a mechanism for slowly but permanently removing covalent crosslinks even from an initially quite strong A70-PLL network.

In this chapter, we study the ability of this system to form a temporary covalently crosslinked interpenetrated network inside the CaAlg composite capsules. CaAlg composite capsules are formed by adding the polyanion, A70, to the sodium alginate solution prior to gelling in calcium chloride. Subsequent exposure of the resulting CaAlg/A70 composite capsules to PLL solutions should lead to a crosslink network. The distribution of this crosslinked network within the capsules depends on molecular weight and mobility of polyelectrolytes in the alginate gel which is studied by CLSM. Hence, fluorescently labelled A70, A70*f*, and rhodamine B labelled PLL, PLLr, were produced and used to make composite capsule. The enamine bond formation and its stability in composite beads were studied by exposing CaAlg composite capsules to 0.1M NaOH.

3.4.1 Study of labelling procedure

The fluorescently labelled A70 was prepared through two different methods: a) labelling in aqueous solution and b) incorporation of a fluorescent monomer during polymerization in an organic environment. Labelling A70 is intended to cause the FITC to be connected directly to the methylene of acetoacetate in the MOEAA unit; however, there are a number of competing processes may occur during labelling:

1. FITC reacts with A70 (Fig. 3.1.B)
2. FITC may hydrolyze to the less fluorescent 5-aminofluorescein especially in basic environment (Figure 3.1. A)[111-113]
3. 5-aminofluorescein may react with A70 (Fig. 3.1.C)

4. The acetoacetate groups may hydrolyze leading to a loss of reactive groups and/or fluorescent label
5. 5-aminofluorescein attached via an enamine may be lost by hydrolysis

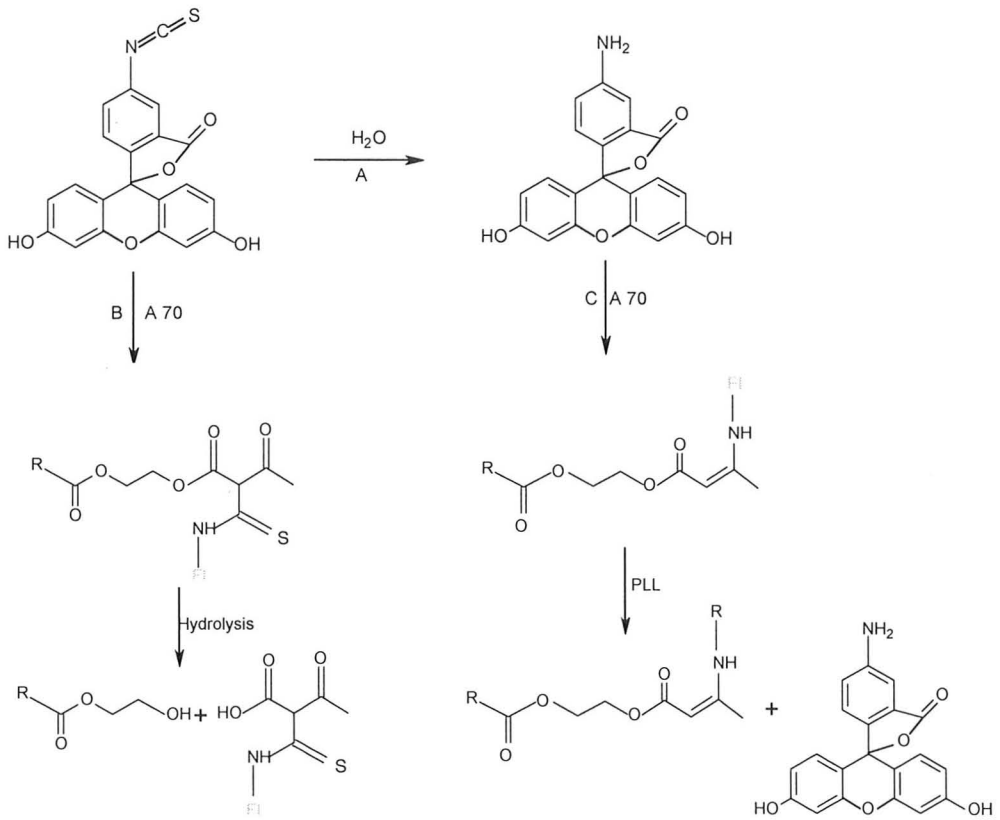

Figure 3.1 **A**) Hydrolysis of FITC to 5-aminofluorescein; **B**) Labelling of A70 by FITC and hydrolysis of labelled product; **C**) Labelling of A70 by 5-aminofluorescein and delabelling by PLL and hydrolysis.

While the UV-Vis analysis showed a degree of labelling of 0.22%, GPC results revealed that just 53% of the fluorescent label was still attached to A70f_{aq}, and 17% of the initial fluorescent material eluted in low molecular weight fractions. ^{1}H-NMR spectra of A70f_{aq} showed that after labelling in aqueous solution 44% of the acetoacetate groups were hydrolyzed (c.f., 12% before labelling), increasing to 64% after 3 months storage of

the solid sample in the fridge. It seems that A70f_{aq} undergoes considerable hydrolysis during and after labelling, which may lead to the loss of the fluorescent label. In addition, optical microscope images showed that A70f_{aq} solutions in the GPC aqueous mobile phase contained aggregated material (Figure 3.2). Therefore, some of the labelled material was lost by filtering the solution before injection into the GPC column.

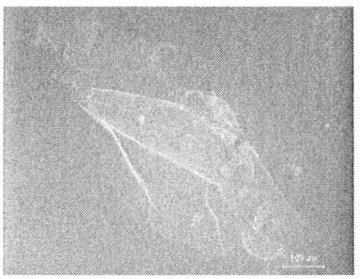

Figure 3.2 Optical microscopy image of A70f_{aq} aggregate in GPC aqueous mobile phase, 10X magnification. Scale bar is 100 μm.

In contrast, the A70f_{org} that was prepared by copolymerizing APM*f* with MAA and MOEAA showed 12% initial hydrolysis, the same level as is seen with unlabelled A70 prepared by copolymerization. Nearly all of the fluorescent label (≥90%) was eluted with the polymeric fraction in GPC indicating that the label remained attached to the polymer. Also, comparing the emission spectra of the two different A70*f* samples revealed higher fluorescence efficiency for A70f_{org} at the same fluorescent concentration due to preventing FITC hydrolysis to 5-aminofluorescein by labelling in organic environment (Figure 3.3).

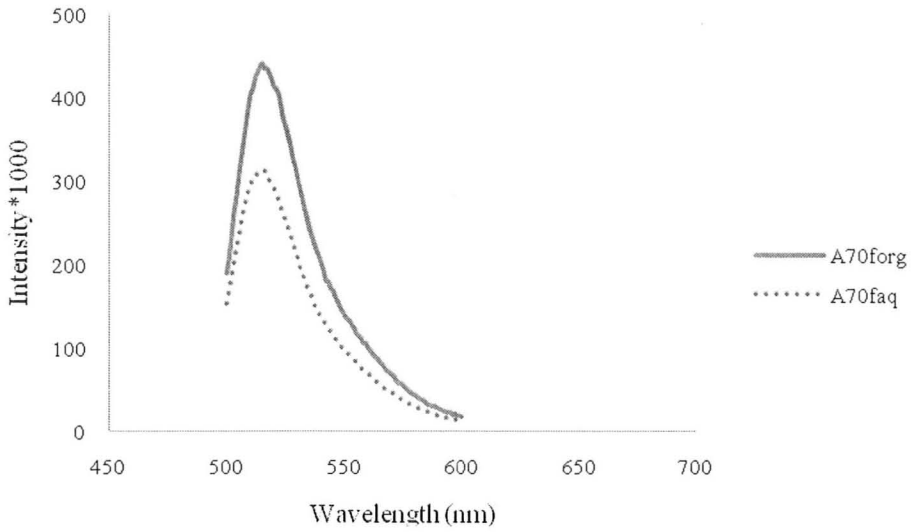

Figure 3.3 Emission spectra of FITC-labeled A70. Absorption adjusted to 0.1 at 488nm (the wavelength of excitation for confocal microscopy) to measure the fluorescent emission intensity of solutions absorbing the same number of photons.

According to these results A70f_{org} was chosen to make composite capsules because the label was attached via a stable linkage, it had higher fluorescence efficiency and had not lost significant fractions of the reactive acetoacetate groups. Through the rest of the thesis A70f_{org} was named A70*f*.

UV-Vis analysis of PLLr showed 0.77% and 0.42% degree of labelling for PLLr at 4-15k Da and 15-30kDa, respectively.

3.4.2 Study of A70 distribution in Ca (Alg/A70 (0.5%)) composite capsule

CaAlg composite capsules containing polyanion (A70) were prepared by extruding the solution containing 1% (or 1.5%) sodium alginate and 0.5 % A70 or A70*f* into the $CaCl_2$ gelling bath. The resulting composite capsules were exposed to different concentrations of PLL, washed with saline and $CaCl_2$ gelling bath solution, and then coated with 0.1% A70 solution (Scheme 3.3). The final capsules had an average diameter

that ranged from 500 to 700 μm depending on the batch with a typical standard deviation of ± 25 μm. The capsules had a smooth surface after coating by A70.

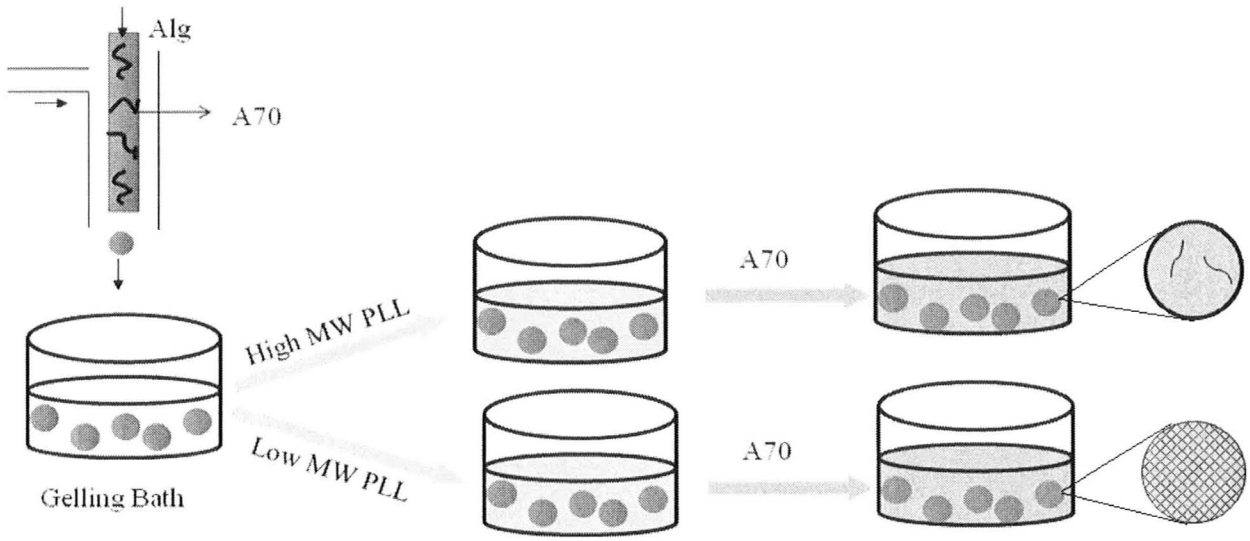

Scheme 3.3 Extrusion method to form core-crosslinked composite capsules.

To determine the fraction of A70 trapped in the CaAlg composite capsules, the supernatant solution used during formation of CaAlg gel and coating with PLL was analyzed by UV-Vis spectroscopy. This study showed that 66.5±1.7 % of the initial A70*f* was trapped in CaAlg gel at either alginate concentration (1 or 1.5%) after gelling, and no significant amounts of A70*f* were lost during the subsequent PLL coating. Thus, A70*f* is lost mostly into the gelling bath while the droplets shrink to about 60% of their original volume.[114, 115]

CLSM images of the CaAlg (1%)/ A70*f* (0.5%) composite capsule showed that A70*f* is initially distributed homogenously within the CaAlg composite capsules. However, the capsules revealed a heterogeneous A70*f* distribution after coating by PLL

4-15 kDa, indicating that A70*f* had become more concentrated at or near the capsule surface (Figure 3.4).

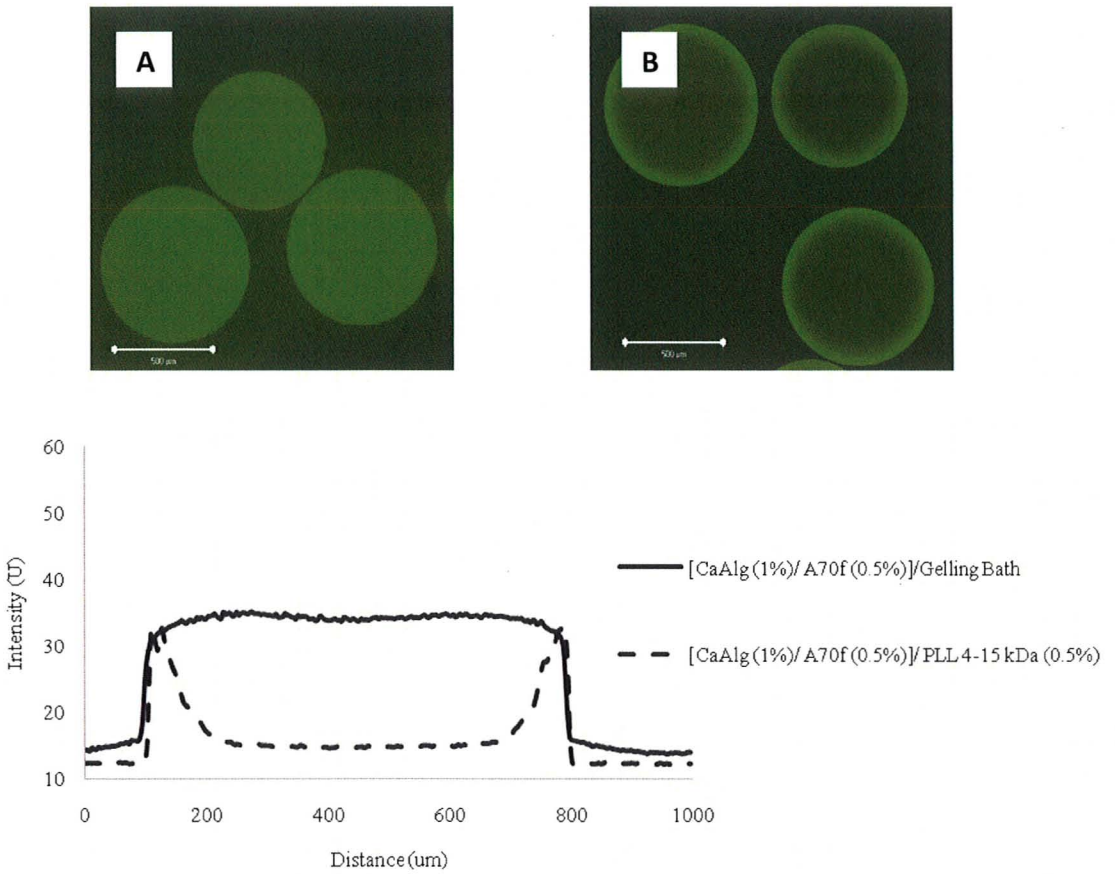

Figure 3.4 *Top*: CLSM equatorial optical sections showing the distribution of A70*f* in CaAlg (1%)/A70f (0.5%) composite capsules at **A**) after gelling; **B**) after coating with PLL 4-15kDa. *Bottom*: Line profiles of images A and B. Scale bar is 500µm.

The polyelectrolyte mobility in CaAlg gel depends on polyelectrolyte MW, interaction of polyelectrolyte with Ca ion and alginate, and the CaAlg pore size. Our previous study showed no microscopic phase separation for A70 solution in the presence of Ca ion, [116] hence we expect that A70 will retain some mobility even in CaAlg gel and its ability to diffuse through the CaAlg gel will be determined by the gel pore size and the

A70 MW. In an attempt to reduce the A70 mobility, the alginate concentration was increased from 1 to 1.5% in hopes of obtaining denser gels that might be better able to trap A70. Once again A70f is homogeneously distributed throughout the CaAlg beads (Fig. 3.5 A). Although, the A70 mobility was diminished in CaAlg (1.5%)/ A70*f* (0.5%) composite capsules but A70 had again migrated to the shell after exposure to PLL 4-15kDa (Fig. 3.4 B), and especially after exposure to PLL 15-30 kDa (Figure 3.5 C).

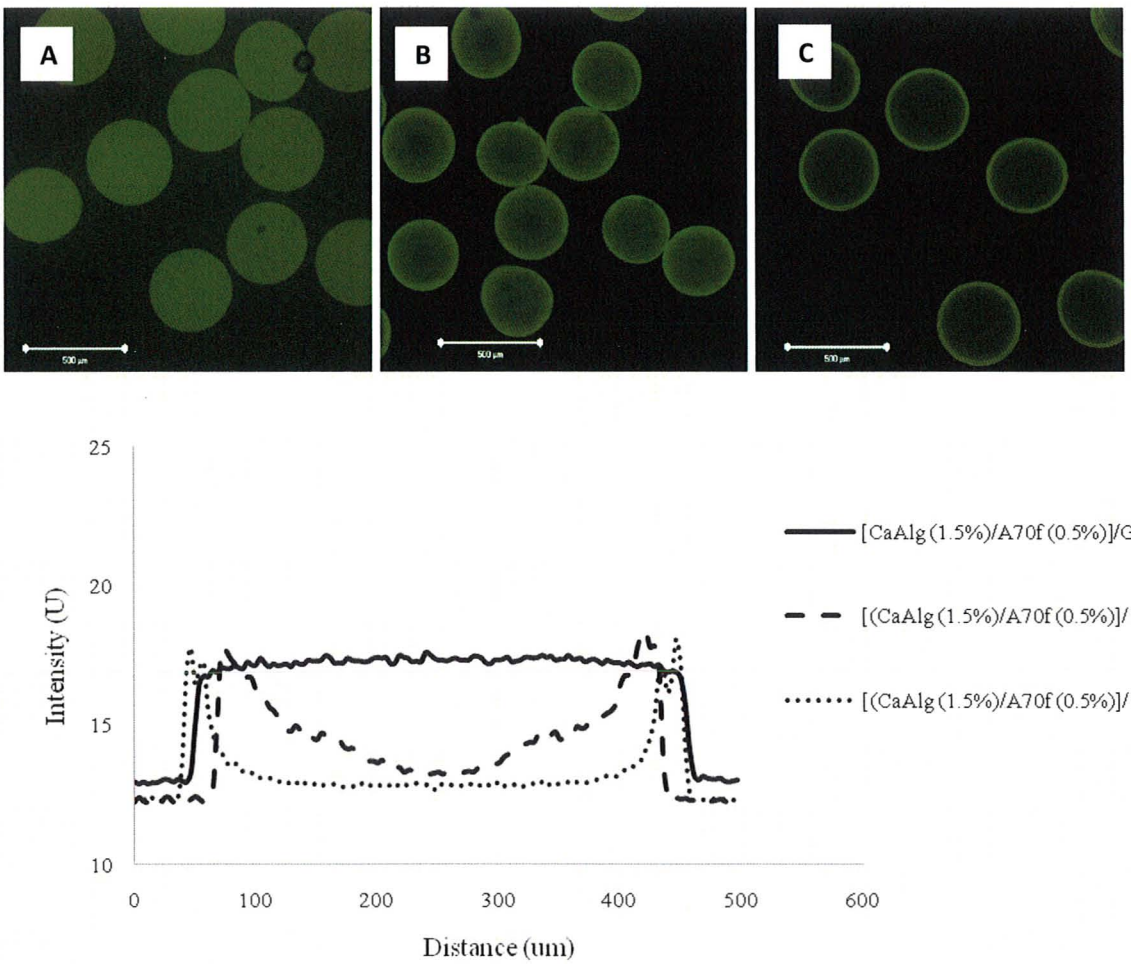

Figure 3.5 *Top*: CLSM equatorial optical sections showing the distribution of A70*f* in CaAlg (1.5%)/A70f (0.5%) composite capsules at **A**) after gelling; **B**) after coating with PLL 4-15kDa; **C**) after coating with PLL 15-30kDa. *Bottom*: Line profiles of images A-C. Scale bar is 500μm.

According to these results a hypothesis is proposed that the A70 becomes more mobile due to a change in the CaAlg gel structure or the interactions of A70 with the gel upon exposure to the coating solution. These changes could take the form of Ca/Na exchange that weakens the gel or the interaction of A70 with the gel, or/and the in-diffusion of PLL and its complexation with alginate may cause a change in gel structure. Once the A70 begins to out-diffuse it will encounter higher PLL concentrations near the capsule surface where it will be captured. To test this hypothesis of A70 mobility, CaAlg (1.5%)/A70*f* (0.5%) capsules were studied by optical microscopy while being exposed to various solutions (section 3.3.3).

3.4.3 Study of A70 mobility inside the CaAlg composite capsule

Below we studied the A70*f* movement in CaAlg (1.5%)/A70*f* (0.5%) composite capsules by fluorescent microscopy. In this method capsules were placed on a microscope slide, covered with a glass cover slip, and examined by fluorescence microscopy at room temperature. The cover slip seals the top and bottom surfaces of the capsules, transforming them into rounded cylinders that permit observation of lateral out-diffusion of the labeled A70*f*. Images were taken every 30 sec and the fluorescence intensity from a representative area in the centre of the bead was measured.[110]

One concern in doing this type of experiment that involves extended exposure of the capsules to light is that photobleaching of the fluorescein chromophores may occur. To test for the occurrence and/or extent of photobleaching over the course of an experiment, capsules were exposed to either continuous or non-continuous irradiation with the exciting light. For non-continuous irradiation the shutter was opened for 3 sec before each image was collected such that the exposure to light was only 4-5 sec per image rather than 30 sec as experienced in the continuous irradiation. The resulting rounded cylinders showed no bleaching under non-continuous light while those that were exposed to continuous irradiation showed a nearly 50% decrease in fluorescence intensity (Figure 3.6, 3.7), thus all further experiments were run under non-continuous irradiation.

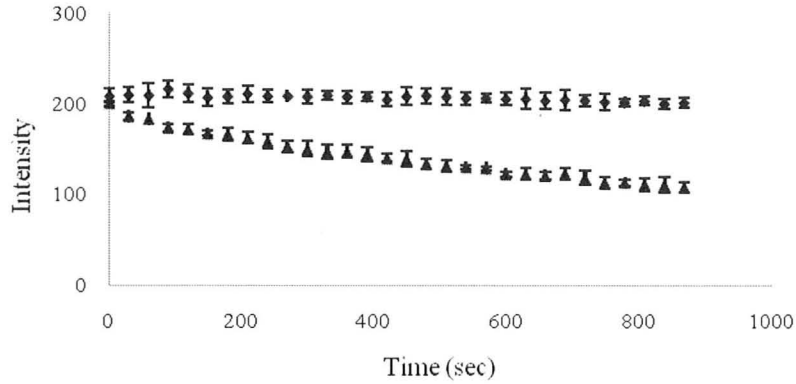

Figure 3.6 Fluorescence intensity in the centre of CaAlg (1.5%)/A70*f* (0.5%) composite beads under (◆): non-continuous microscopy light, (▲: continuous microscopy light.

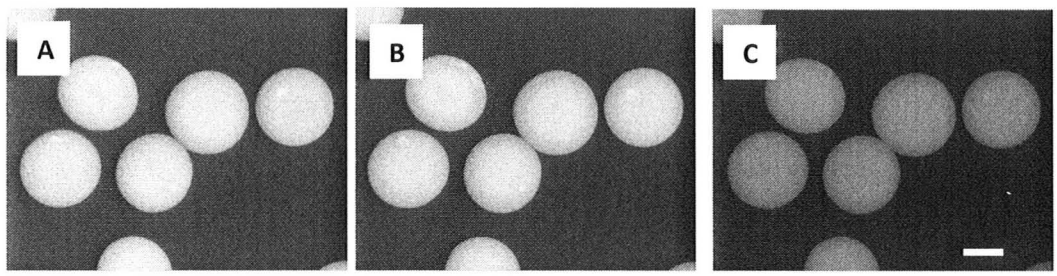

Figure 3.7 Fluorescence microscopy images of CaAlg (1.5%)/A70*f* (0.5%) composite capsules **A**) before irradiation; **B**) after 15 min of non-continuous light, **C**) After 15min of continuous light, 5X, Scale bar is 200µm.

CaAlg (1.5%)/A70*f* (0.5%) composite capsules were washed two times with saline, and then covered by glass cover slip while immersed in saline. Figure 3.8 shows a decrease in fluorescence intensity at the capsule centre, due to a combination of known bead swelling and out-diffusion. The remaining A70f is still homogenously distributed within the beads (Figure 3.9 A, B).

To study the effect of PLL 15-30 kDa on A70*f* distribution the composite capsules were washed two times with saline, and then exposed to PLL while covered with a cover slide. They were then observed while still exposed to this PLL solution. The rate of decrease of the fluorescence intensity at the capsule centre was very similar to that of the capsules that had been exposed to just saline (Figure 3.8), but the capsules showed a heterogeneous A70*f* distribution (Figure 3.9 D). These findings show that PLL can trap A70 near the shell, leading to a heterogeneous A70*f* distribution.

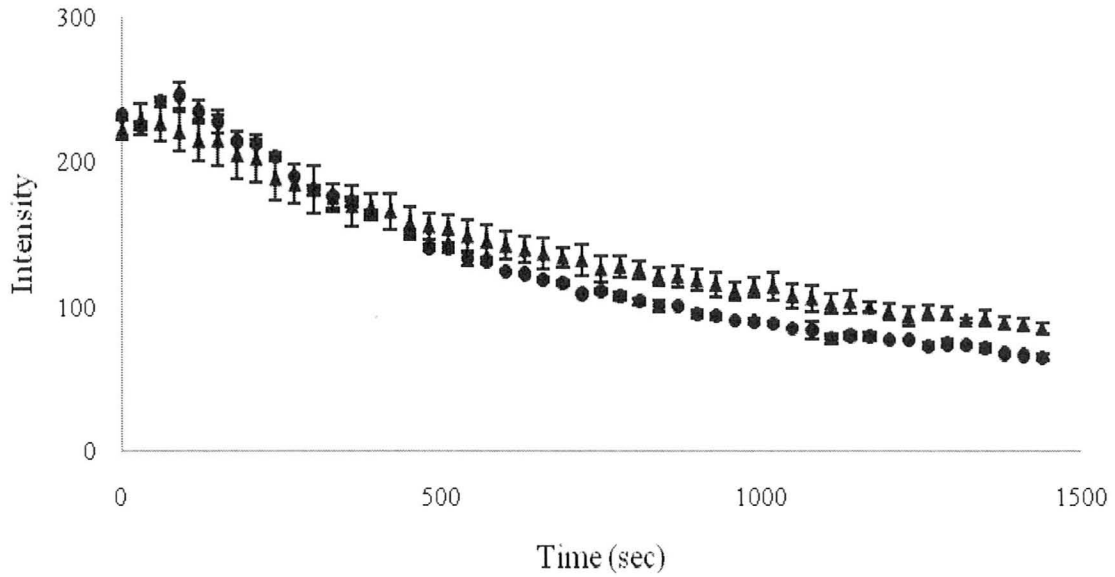

Figure 3.8 Change in fluorescence intensity in the centre of CaAlg (1.5%)/A70*f* (0.5%) composite capsules with time in: (▲) saline, or (●) 0.5% PLL (15-30 kDa) in saline.

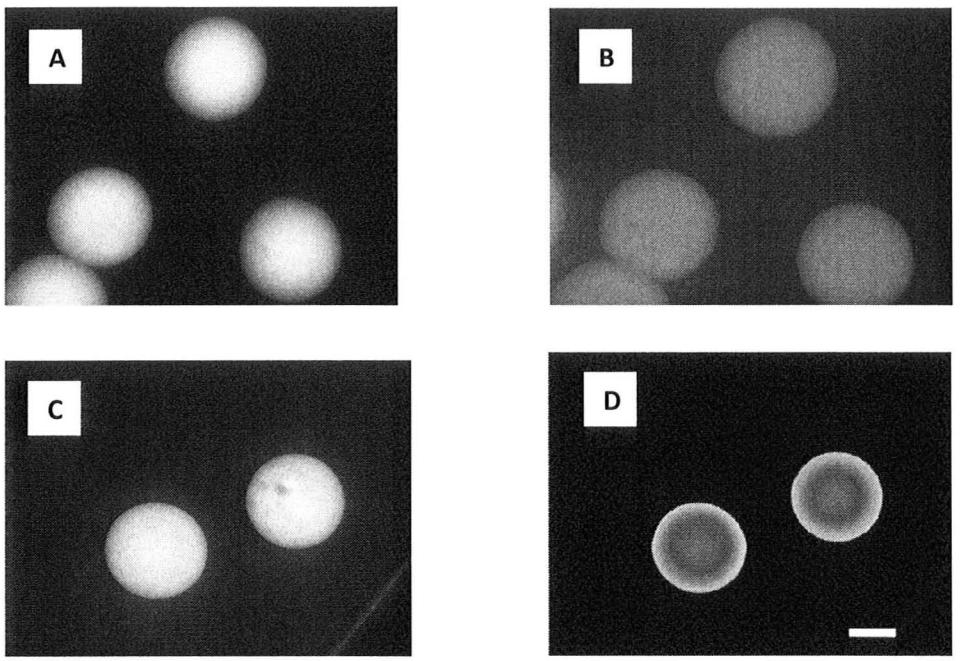

Figure 3.9 Optical microscopy images of CaAlg (1.5%)/A70*f* (0.5%) composite capsules under non-continuous light , **A**) 2 times washing with saline and immediately after covering; **B**) 25 min after A; **C**) 2 times washed twice with saline before 0.5% PLL solution was added, immediately after covering; **D**) 25 min after C, 5X, Scale bar is 200μm.

To distinguish the effect of ionic interaction on polyanion distribution from the covalent bonds, composite capsules were made with CaAlg (1.5%)/A100*f* (0.5%), FITC-labelled poly methacrylic acid solution. The resulting capsules showed heterogeneous A100*f* distribution after exposure to PLL 15-30 kDa (Figure 3.10). This shows that opposite diffusion and polyelectrolyte complexation is responsible for this trapping of A100*f* and presumably A70*f* near the shell.

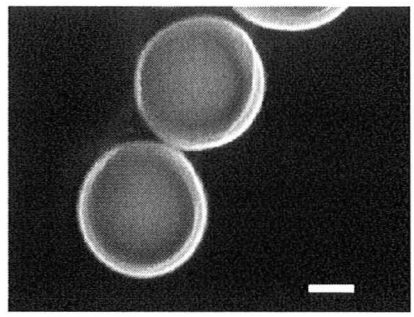

Figure 3.10 Optical microscopy image of the CaAlg (1.5%)/A100*f* (0.5%) composite capsules after 2 times washing with saline and injecting 0.5% PLL 15-30 kDa, Scale bar is 200μm.

3.4.4 Study of PLL distribution in Ca (Alg/A70 (0.5%)) composite capsule

To study the diffusion distance of PLL the (CaAlg (1%)/ A70*f* (0.5%)) composite capsules containing A70 in the core were coated with different concentrations of RITC-labelled PLL (PLLr) solution of 4-15 kDa and 15-30 kDa MW, and studied by optical microscope, CLSM and UV-Vis spectroscopy. The diameter of the capsules depends on exposure time, [114] and PLL concentration. In our study increasing the PLL concentration at the same exposure time shrank the capsules by up to 10-15% of diameter.[115-116]

The UV/ Vis analysis of the supernatant after coating with PLLr showed that the amount of PLL bound to the capsules increased with PLL concentration for both PLL MWs. CLSM of capsules coated with PLLr 15-30 kDa revealed that the bound PLL is concentrated in the 15 to 34 micron outer shell (Figure 3.11). In contrast, PLL 4-15 kDa could diffuse further into the core and by increasing the concentration of PLL solution, more PLL was absorbed and the thickness of the PLL layer was increased (Figure 3.12).

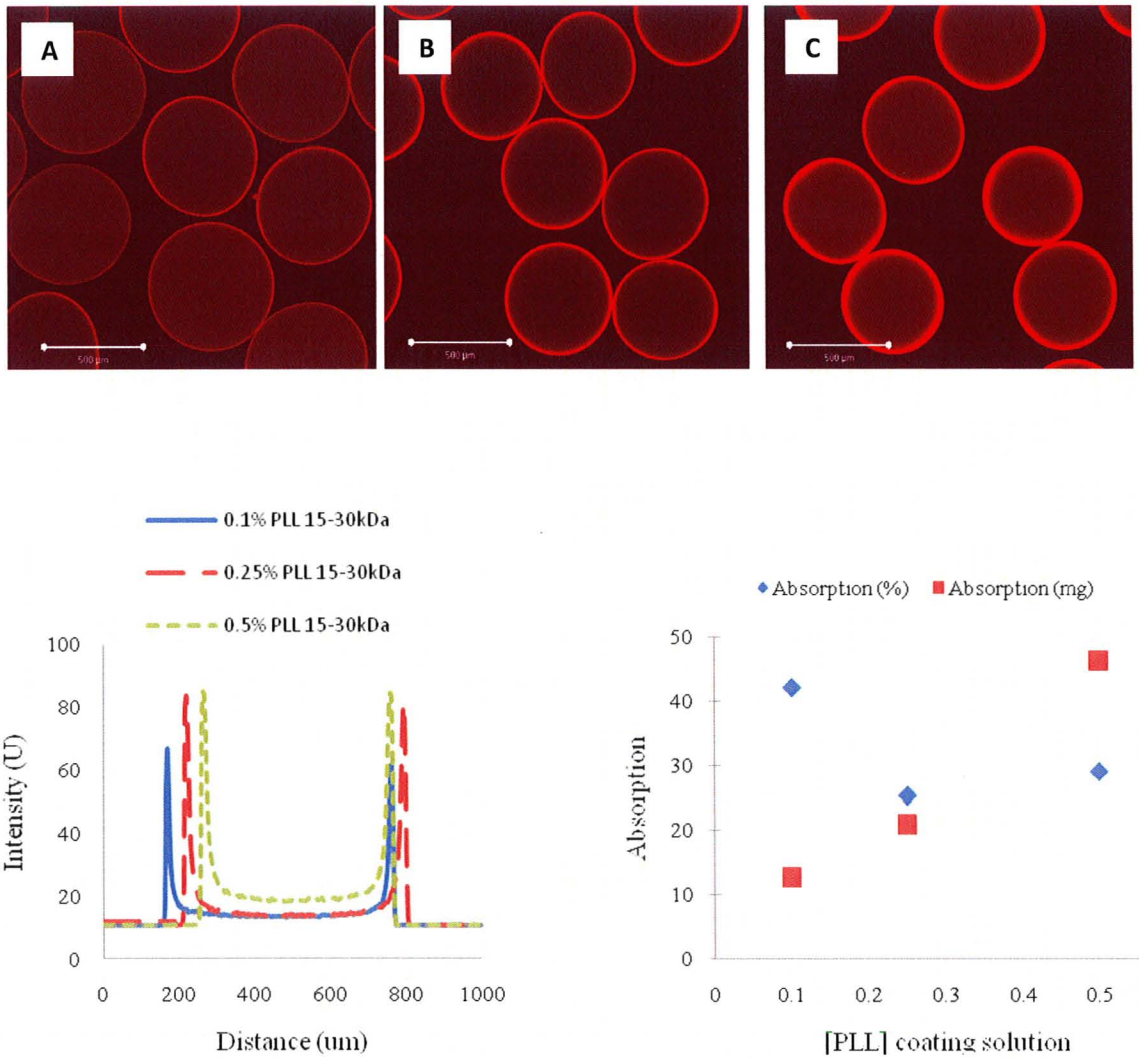

Figure 3.11 *Top*: CLSM equatorial optical sections of CaAlg (1%)/A70 (0.5%)/PLL/A70 (0.1%) composite capsules made with PLL*r* of 15-30 kDa at **A**) 0.1% PLL; **B**) 0.25%; **C**) 0.5% A70. *Bottom*: (Left) Line profiles, (right) PLL absorption based on 750mg PLL coating solution; of images A-C. Scale bars are 500 µm.

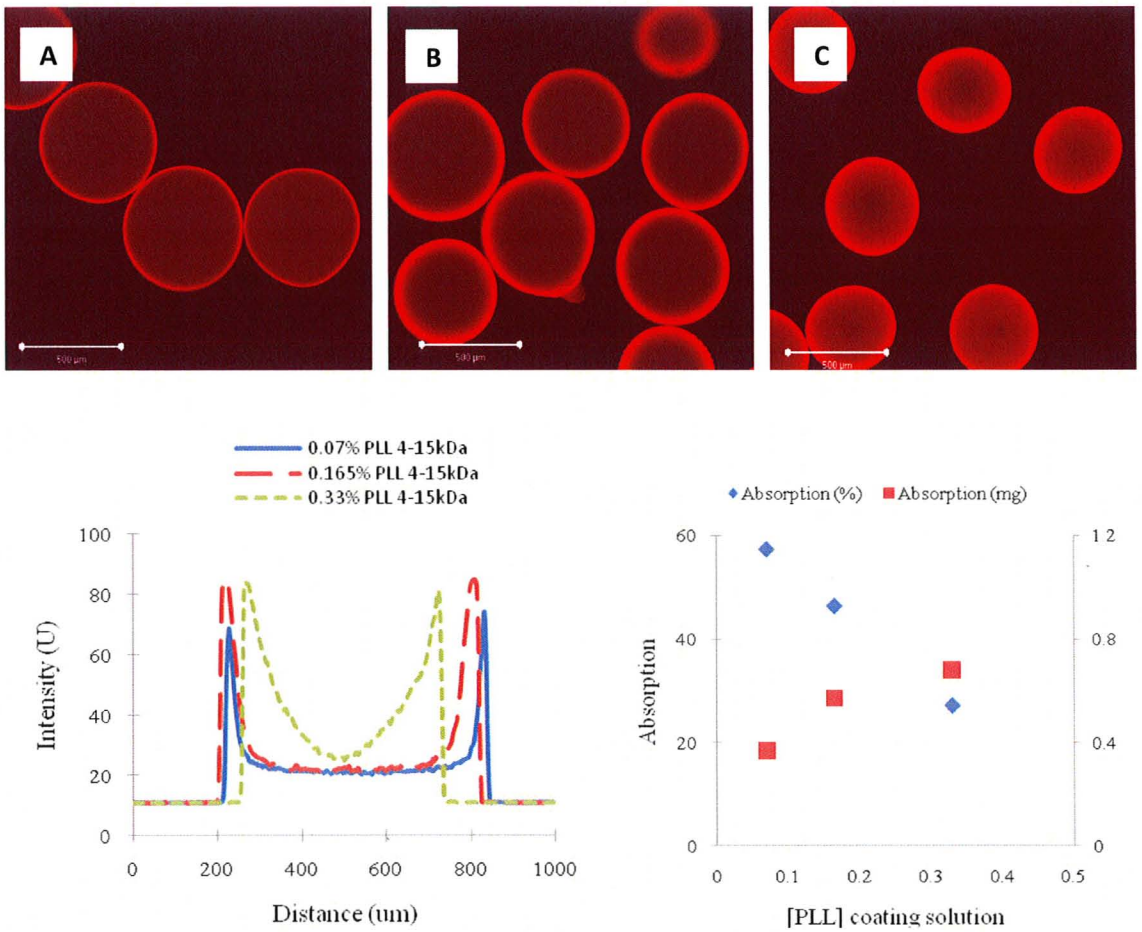

Figure 3.12 *Top*: CLSM equatorial optical sections of CaAlg (1%)/A70 (0.5%)/PLL/A70 (0.1%) composite capsules made with PLL*r* of 4-15 kDa at **A**) 0.07% PLL; **B**) 0.165%; **C**) 0.33%. *Bottom:* (Left) Line profiles, (right) PLL absorption based on 750mg coating solution; of images A-C. Scale bars are 500µm.

A parallel study to make shell crosslinked capsules without A70 in core done by R. Kleinberger in our group showed PLL 15-30 kDa can diffuse completely into the core. This data (shell crosslinked capsules) confirms that a dense shell made between A70 in the core and in-diffusing PLL, limits further in-diffusion of the higher MW PLL.

3.4.5 Chemical study of crosslinked network inside the composite capsule

For the CaAlg (1%)/A70 (0.5%) composite capsules that trapped 66.5% of their original A70 loading, using a more concentrated PLL coating solution leads to higher ratio of crosslinking groups (amine/acetoacetate). Thus we expect more enamine bonds are formed by increasing PLL concentration.

Higher MW PLL (15-30kDa) is concentrated near the shell and does not diffuse into the core as much as lower MW PLL. This indicates that the effective amine/acetoacetate in the core is lower for PLL 15-30 kDa than for PLL 4-15 kDa. In this situation if PLL 4-15 kDa chains are long enough they can form an interpenetrating crosslinked network with A70 in the CaAlg composite core. The possibility of forming enamine bonds and their stability at physiological temperature were studied by challenging capsules with a) 70mM citrate and b) 0.1M NaOH. First composite capsules were exposed to 70mM citrate to extract Ca ions, and the resulting hollow capsules were stored at 37°C. The stability of enamine bonds in aqueous environment at elevated temperature was studied by exposing hollow capsules to 0.1M NaOH (pH ~13) over time and measuring their diameter. At pH~13 the electrostatic network between A70 and PLL cleaves because of the low degree of charge of PLL.[117-118] Thus capsules are maintained just by covalent bond.

This experiment showed that the amount of covalent bonds decreased over time due to continued hydrolysis of the enamine and ester groups, and the diameter of the composite capsules increased for both high and low MW PLL (Figure 3.13, 3.14). Capsules formed with low MW PLL dissolved in 0.1M NaOH after 5-28 days storage at 37°C in saline, depending on PLL concentration (Figure 3.13), while the beads formed with higher MW PLL all survived for at least 28 days (Figure 3.14). These results seemed to indicate that while low MW PLL can diffuse further into the core, it cannot crosslink as effectively as high MW PLL, and just a thin and weak crosslinked shell formed. It

appears that beads formed with higher MW PLL are stronger, though they may only form crosslinked shells, and not the desired core-crosslinked capsules.

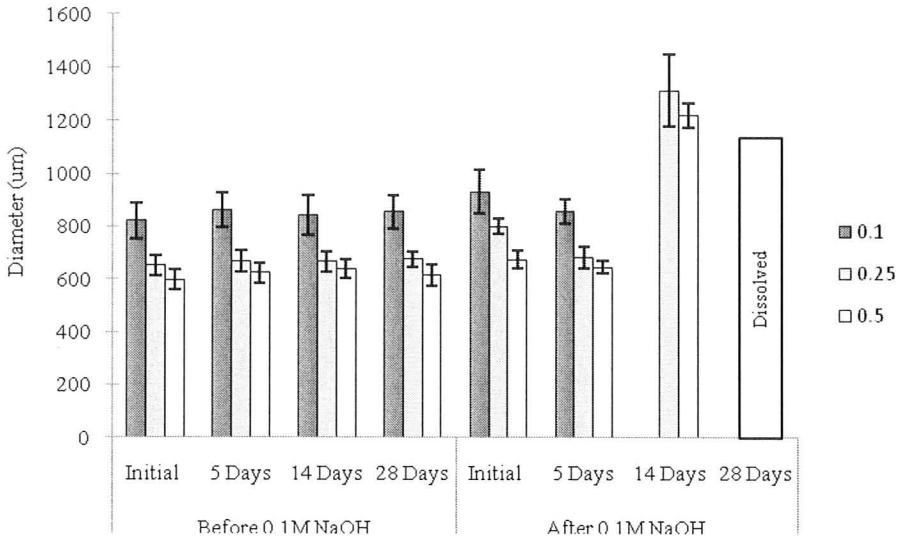

Figure 3.13 Chemical stability of CaAlg (1%)/A70 (0.5%)/PLL4-15 kDa/0.1% A70 capsules at 37°C in saline.

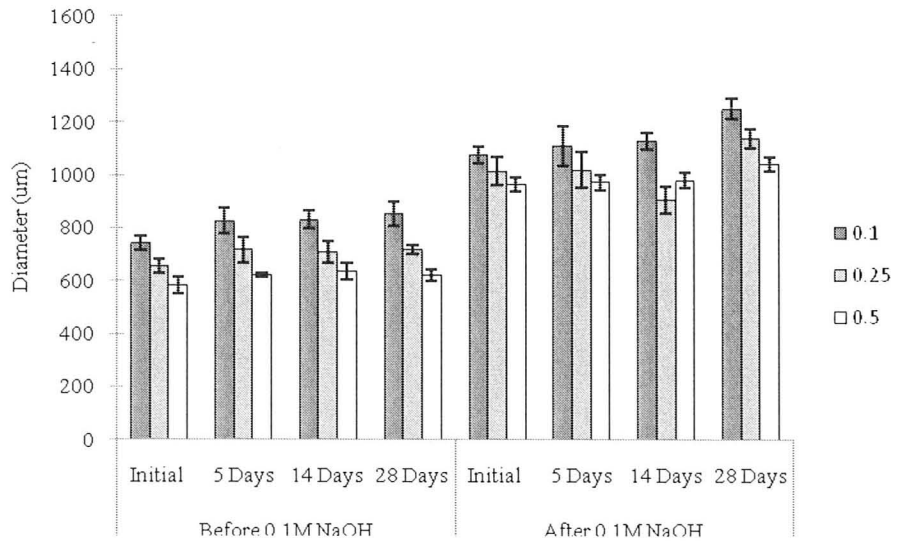

Figure 3.14 Chemical stability of CaAlg (1%)/A70 (0.5%)/PLL15-30 kDa/0.1% A70 capsules at 37°C in saline.

The model studies described in Chapter 2 showed that the enamine bond is reversible and has a short life time in aqueous environment, but the polydentate nature is expected to help keep the network in capsules. However the network does degrade due to the continuous A70 hydrolysis.

Exposing capsules made with higher Alg concentration [CaAlg (1.5%)/ A70 (0.5%)] to 70mM citrate and 0.1M NaOH also revealed that no crosslinked network was formed in CaAlg core at even 1.5% alginate concentration (Figure 3.15). While this represents a new approach to form shell-crosslinked capsules, it still leaves open the question of how one could form core-crosslinked capsules.

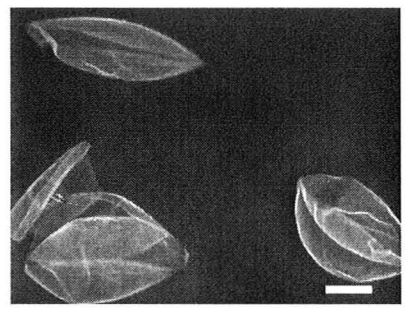

Figure 3.15 Optical microscopy image of [CaAlg (1.5%)/A70f (0.5%)] composite capsules coated with 0.5% PLL 4-15kDa, after exposure to 70mM citrate and 0.1M NaOH, 5X, Scale Bar is 200μm.

The previous results reported by J. Mazumder showed homogenous distribution for A70 in the CaAlg core made using 1% Kelton LVCR (40% G), and interpenetrating cross-linked network for PLL 4-15kDa. These results are in contrast with our samples showing heterogeneous A70 distribution in the capsules without efficient crosslinking in the core. Studies of the diffusion of various size proteins have shown higher diffusion coefficient for the CaAlg capsules formed by high-G content than the high-M content ones, indicating a more porous and open CaAlg network in the high-G gels. [119-121]Thus

the resulting big pores and open structure are probably the reason why A70 is too mobile in the capsules formed with high-G content alginate (Pronova UP MVG, ≥60% G).

3.5 Conclusion

In this study a new method was studied based on inclusion of A70 in CaAlg core to reinforce the conventional APA capsules by forming core-crosslinked core. The distribution of polyelectrolytes was studied by mapping fluorescently labelled analogs with CLSM. While A70 showed initial homogenous distribution as capsules formed in gelling bath, it was distributed heterogeneously after coating with PLL. Study of A70 mobility in Alg gel confirmed that opposite diffusion of polyelectrolytes and polyelectrolyte complexation are responsible for trapping of A70 near the shell. The depth of PLL penetration studied by varying PLL MW and concentration showed that PLL can diffuse further into the core at lower MW and higher concentration. However exposing the resulting capsules to 70mM citrate and 0.1M NaOH demonstrated no effective crosslink bonds formed in the CaAlg core. According to these results the mobility of A70 in the porous alginate hydrogel is high and leads to formation of a dense shell which interferes with PLL diffusion at higher MW, limiting the possibility of forming covalent bonds in the core.

Study of the stability of the enamine-crosslinked network at physiological condition (37°C, in saline at pH~7) revealed slow but permanent enamine bond cleavage over time. These results are comparable with our previous study of enamine bond stability in model systems (Chapter 2). This positions A70 as crosslinkable material to form a temporarily networks with a significant interest to protect encapsulated cells just for the time needed to develop their own extracellular matrix, and as such can certainly find valuable uses in the field of cell encapsulation.

Chapter 4: Conclusion and Future Work for Cell Encapsulation

4.1 Conclusion

The chemical structure of polyanion, its hydrolysis rate, enamine bond formation between acetoacetate and amine and the enmaine bond stability under physiological condition in different molecule models and capsules were studied as summarized below:

1. The HEMA was likely formed by hydrolysis of MOEAA before, during or after polymerization and the HEMA content corresponds to a 12% degree of MOEAA hydrolysis. Study the hydrolysis rate of A70 in aqueous solutions showed that A70 loses its functional group (acetoacetate) during the dissolution process at basic condition. Fortunately, we could survive most of the acetoacetate groups using an improved method for dissolving A70 that largely avoids temporary excursions to high pH, and thus limits the initial hydrolysis. However, hydrolysis continues over time at neutral pH, leading to near complete hydrolysis after 30 days at 40°C.
2. The enamine bond formation in organic and aqueous environment via different molecular models showed low level enamine bond for the small molecule and polymer-small molecule model in aqueous environment. The enamine bond level improves in polymer-polymer model in aqueous environment due to the hydrophobic environment formed by the electrostatic interaction between PLL and A70, and higher concentration of reactants. However the covalent bonds slowly but permanently cleave at physiological pH and temperature. This means that the combination of enamine reversibility and acetoacetate hydrolysis creates a mechanism for slowly but permanently removing covalent crosslinks even from an initially quite strong A70-PLL network. In turn, this implies that these networks, in contrast to those formed using more permanent amide-based crosslinks, should be considered to be temporary networks with a significant

potential for applications that require protection of cells just for the time needed to develop their own extracellular matrix, and as such can certainly find valuable uses in the field of cell encapsulation.

3. We have re-investigated a new method based on inclusion of A70 in CaAlg core to reinforce the conventional APA capsules by forming core-crosslinked capsule. The distribution of polyelectrolytes studied by mapping fluorescently labelled analogs with CLSM showed an initial homogenous distribution for A70 chains in the CaAlg core as capsules formed in gelling bath. A70 was distributed heterogeneously after coating with PLL. Study of A70 mobility in Alg gel revealed that opposite diffusion of polyelectrolytes and polyelectrolyte complexation are responsible for trapping of A70 near the shell. The depth of PLL penetration studied by varying PLL MW and concentration showed that PLL can diffuse further into the core at lower MW and higher concentration. However exposing the resulting capsules to 70mM citrate and 0.1M NaOH demonstrated no effective crosslink bonds formed in the CaAlg core. According to these results the mobility of A70 in the porous alginate hydrogel and producing a dense shell which limits the PLL diffusion at higher MW, limits the possibility of forming covalent bonds in the core. These results contradict J. Mazumder's previous results showed homogenous distribution for A70 in the CaAlg core made using 1% Kelton LVCR (40% G), and interpenetrating cross-linked network for PLL 4-15kDa. The main reason showed this difference is forming bigger pores and more open CaAlg structure by using high-G content alginate (Pronova UP MVG, ≥60% G) which leads to high A70 mobility within CaAlge gel.

4. Study of the stability of the enamine-crosslinked network at physiological condition (37°C, in saline at pH~7) revealed slow but permanent enamine bond cleavage over time. These results are comparable with our previous study of enamine bond stability in model systems. This positions A70 as crosslinkable material to form a temporarily crosslinked network with a significant interest to

protect encapsulated cells just for the time needed to develop their own extracellular matrix.

4.2 Future Work

Future work in the area of covalently core-crosslinked CaAlg capsules may involve fundamental research on the life time of covalent bond under physiological condition, providing a homogenous distribution of covalent bond inside the CaAlg core, and study of the biocompatibility of resulting capsules.

According to the results of this thesis the enamine bond level in aqueous environment increases by forming PEC complexation; however, the continuous hydrolysis of acetoacetate group of A70 provides a temporary covalently crosslinked network with about one month life time. In order to increase the life time of a covalently crosslinked network two scenarios may be considered as below:

1. Replacement of acetoacetate ester group of A70 with acetoacetamide functional group to diminish the hydrolysis rate of polyanion
2. Providing more stable categories of covalent bonds such as amide, urea, thioester, and thiourea to control the reversibility of the covalently crosslinked network in aqueous environment.[87, 88]

One of the thesis goals was forming core-crosslinked CaAlg capsules by spreading polyelectrolytes homogenously inside the capsule. According to our results the polyelectrolyte distribution was affected strongly by the mobility of polymer chains in porous hydrogel. As polyanion migrates to the shell and form PEC complexation with pioneer diffused PLL chains, it limits further diffusion of higher MW PLL chains. Thus, one of the next steps may be controlling the mobility of polyanion in CaAlg core. To address this issue, polyanions at higher MW and lower PDI will be prepared which may reduce the mobility of polyanion in the CaAlg core.

This thesis also aimed to improve the biocompatibility of APA capsules. In order to study the effect of polyanion on biocompatibility, the protein absorption of synthetic polymers should be studied under *in vivo* and *in vitro* conditions. Also the interaction between crosslinking efficiency and cell growth will be studied as the highly crosslinked hydrogel may cause lack of capacity of dividing for cells, and hard oxygen and nutrients access.[122] For this purpose the cell growth in core-crosslinked CaAlg capsules will be compared with non-crosslinked ones and common APA capsules.

Reference

1. R. P. Lanza, W. L. Chick. Transplantation of encapsulated cells and tissues. *Surgery*, 1997, *121* (1), 1-9.
2. W. M, Kuhtreiber, R. P. Lanza, W. L. Chick. Cell encapsulation technology and therapeutics. A Birkhauser Boston Product. 1999, 3
3. R. H. Li. Materials for immunoisolated cell transplantation. *Advanced Drug Delivery Reviews*. 1998, *33*. 87-109.
4. P. J. Morris. Immunoprotection of therapeutic cell transplants by encapsulation. *Trends Biotechnol*. 1996, *14*, 163-167.
5. B. Rihova. Immunocompatibility and biocompatibility of cell delivery systems. Advanced *Drug Delivery Reviews*. 2000, *42*, 65-80.
6. A. Murua, A. Portero, G. Orive, R.M. Hernandez, M.D. Castro, J.L. Pedraz. Cell microencapsulation technology: towards clinical application. *Journal of Controlled Release*. 2008, *132*,76-8
7. P. Aebischer, M. Scluep, N. Deglon, J. M. Joseph, L. Hirt, B. Heyd, M. Goddard, J. P. Hammang, A. D. Zurn, A. C. Kato, F. Regli, E. F. Baetge. Intrathecal delivery of CNTF using encapsulated genetically modified xenogeneic cells in amyotrophic lateral sclerosis patients. *Nature Medicine*. 1996, *2*, 696-699.
8. R. P. Lanza, J. L. Hayes, W. L. Chick. Encapsulated cell technology. *Nat. Biotechnol*. 1996, *14*, 1107-1111.
9. P. E. Lacy. Treating diabetes with transplanted cells. *Sci. Am*. 1995, *273*, 50-51, 54-58.
10. H. Uludag, P. Vos, P.A. Tresco. Technology of mammalian cell encapsulation. *Advanced Drug Delivery Reviews*. 2000, *42*, 29-64
11. J. M. Rabanel, X. Banquy, H. Zouaoui, M. Mokhtar. Progress technology in microencapsulation methods for cell therapy. *Biotechnol. Prog*. 2009, *25* (4), 946-963.

12. P. DeVos, B. DeHaan, J. Pater, R. Van Schilfgaarde. Association between capsule diameter, adequacy of encapsulation, and survival of microencapsulated rat islet allografts. *Transplantation*.1996, *62*, 893-899.

13. R. Robitaille, J. F. Pariseau, F. A. Leblond, M. Lamoureux, Y. Lepage, J. P. Halle. Studies on small (350 μm) alginate-poly-L-lysine microcapsules. III. Biocompatibility of smaller versus standard microcapsules. *J Biomed Mater Res A*. 1999, *44*, 116-120.

14. A. Omer, V. Duvivier-Kali, J. Fernandes, V. Tchipashvili, C. K. Colton, G. C. Weir. Long-term normoglycemia in rats receiving transplants with encapsulated islets. *Transplantation*. 2005, *79*, 52-58.

15. B. A. Zielinski, P. Aebischer. Chitosan as a matrix for mammaline cell encapsulation. *Biomaterials*. 1994, *15*, 1049-1056.

16. J. E. Babensee. U. De Boni. M.V. Sefton. Morphological assessment of hepatoma cells (HepG2) microcapsulated in a HEMA-MMA copolymer with and without matrigel. *J. Biomed. Mater. Res.* 1992, *26,* 1401-1418.

17. A. S. Hoffman. Hydrogels for biomedical applications. *Advanced Drug Delivery Reviews*. 2002, *54*, 3-12.

18. S. Sakai, K. Kawakami. Both ionically and enzymatically crosslinkable alginate-tyramine conjugate as materials for cell encapsulation. *J Biomed Mater Res A*. 2008, *85*, 345-351.

19. C. Schwinger, A. Klemenz, K. Busse, J. Kressler. Encapsulation of living cells with polymeric systems. *Macromolecular Symposia*. 2004, *210*, 493-499.

20. D. Poncelet. Production of alginate beads by emulsification/internal gelation. Ann *N Y Acad Sci*. 2001, *944*, 74-82.

21. C. P. Reis, R. J. Neufeld, S. Vilela, A. J. Ribeiro, F. Veiga. Review and current status of emulsion/dispersion technology using an internal gelation process for the design of alginate particles. *J Microencaps*. 2006, *23*, 245-257.

22. B. Strand, Y. A. Morch, G. Skjak-Braek. Alginate as immobilization matrix for cells. *Minerva Biotec*. 2000, *12*, 223-233.

23. C. Schwinger, A. Klemenz, K. Busse, J. Kressler. Encapsulation of living cells with polymeric systems. *Macromolecular Symposia.* 2004, *210*, 493-499.

24. S. Sugiura , T. Oda, Y. Aoyagi, R. Matsuo, T. Enomoto, K. Matsumoto, T. Nakamura, M. Satake, A. Ochiai, N. Ohkohchi, M. Nakajima. Microfabricated airflow nozzle for microencapsulation of living cells into 150 micrometer microcapsules. *Biomed Microdevices.* 2007, *9*, 91-99.

25. J. P. Halle. F. A. LeBlond, J. F. Pariseau. P. Jutras. M. L. Brabant. Y. Lepage. Studies on small (less than 300μm) microcapsules. 2. Parameters governing the production of alginate beads by high-voltage electrostatic pulses. *Cell Transplantation*, 1994, *3*(5), 356-72.

26. G. Langlois, J. Dusseault, S. Bilodeau, S. K. Tam, D. Magassouba, J.P. Halle. Direct effect of alginate purification on the survival of islets immobilized in alginate-based microcapsules. *Acta Biomaterialia.* 2009, *5*, 3433–3440.

27. M. F. A. Goosen, A. S. Al-Ghafri, O. El Mardi, M. I. J. Al-Belushi, H. A. Al-Hajri, E. S. E. Mahmoud, E. C. Consolacion. Electrostatic droplet generation for encapsulat ion of somatic tissue: Assessment of high-voltage power supply. *Biotechnol. Prog.* 1997, *13*, 497–502.

28. K.T. Nijenhuis. Thermoreversible gels. *Adv Polym Sci.* 1987, *136*, 194-202.

29. H. Gin, B. Dupuy, C. Baquey, D. Ducassou, J. Aubertin. Agarose encapsulation of islets of Langerhans: reduced toxicity in vitro. *J Microencaps.* 1987, *4*, 239-242.

30. H. Iwata, H. Amemiya, T. Matsuda, H. Takano, R. Hayashi, T. Akutsu. Evaluation of microencapsulated islets in agarose gel as bioartificial pancreas by studies of hormone secretion in culture and by xenotransplantation. *Diabetes.* 1989, *38*(1), 224-225.

31. H. Iwata, T. Takagi, H. Amemiya, H. Shimizu, K. Yamashita, K. Kobayashi, T. Akutsu. Agarose for a bioartificial pancreas. *J Biomed Mater Res A.* 1992, *26*, 967-977.

32. O. J. Cayre, P. F. Noble, V. N. Paunov. Fabrication of novel colloidosome microcapsules with gelled aqueous cores. *Journal of Materials Chemistry*. 2004, *14*, 3351-3355.

33. H. Iwata, T. Takagi, H. Amemiya. Agarose microcapsule applied in islet xenografts (hamster to mouse). *Transplant Proc*. 1992, *24*, 952.

34. H. Iwata, K. Kobayashi, T. Takagi, T. Oka, H. Yang, H. Amemiya, T. Tsuji, F. Ito. Feasibility of agarose microbeads with xenogeneic islets as a bioartificial pancreas. *J Biomed Mater Res A*. 1994, *28*, 1003-1011.

35. Y. Miyoshi, I. Date, T. Ohmoto, H. Iwata. Histological analysis of microencapsulated dopamine-secreting cells in agarose/poly(styrene sulfonic acid) mixed gel xenotransplanted into the brain. *Exp Neurol*. 1996, *138*, 169-175.

36. T. Kin, H. Iwata, Y. Aomatsu, T. Ohyama, H. Kanehiro, M. Hisanaga, Y. Nakajima. Xenotransplantation of pig islets in diabetic dogs with use of a microcapsule composed of agarose and polystyrene sulfonic acid mixed gel. *Journal of Neuroendocrine Tumors and Pancreatic Diseases and Sciences*. 2002, *25* (1), 94-100.

37. R. Suzuki, Y. Yoshioka, E. Kitano, T. Yoshioka, H. Oka, T. Okamoto, N. Okada, Y. Tsutsumi, S. Nakagawa, J. Miyazaki, H. Kitamura, T. Mayumi. Development of a novel cytomedical treatment that can protect entrapped cells from host humoral immunity. *Cell Transplant*. 2002, *11*, 787-797.

38. K. Jain , H. Yang, B. R. Cai, B. Haque, A.I. Hurvitz, C. Diehl, T. Miyata, B.H. Smith, K. Stenzel, M. Suthanthiran, A.L. Rubin. Retrievable, replaceable, macroencapsulated pancreatic islet xenografts. Long-term engraftment without immunosuppression. *Transplantation*. 1995, *59*, 319-324.

39. A. Batorsky, J. Liao, A. W. Lund, G. E. Plopper, J. P. Stegemann. Encapsulation of adult human mesenchymal stem cells within collagen-agarose microenvironments. *Biotechnology and Bioengineering*. 2005, *92*(4), 492-500.

40. H. F. Lu, E. D. Targonsky, M. B. Wheeler, Y. L. Cheng. Thermally induced gelable polymer networks for living cell encapsulation. *Biotechnol Bioeng*. 2007, *96*, 146-155.

41. M. Kierstan, C. Bucke. The immobilization of microbial cells, subcellular organelles, and enzymes in calcium alginate gels. *Biotechnol Bioeng*. 1977, *19*, 387-397.

42. T. Zekorn, U. Siebers, A. Horcher, R. Schnettler, G. Klock, R.G. Bretzel, U. Zimmermann, K. Federlin. Barium-alginate beads for immunoisolated transplantation of islets of Langerhans. *Transplant Proc*. 1992, *24*, 937-939.

43. E. P. Herrero, E. M. M. Del Valle, M. A. Galan. Immobilization of mesenchymal stem cells and monocytes in biocompatible microcapsules to cell therapy. *Biotechnol Prog*. 2007, *23*, 940-945.

44. D. A. Rees. Structure, conformation and mechanism in the formation of polysaccharide gels and networks. *Adv.Carbohydr.Chem.Biochem*. 1970, *24*, 267-332.

45. G. T. Grant, E. R. Morris, A. D. Rees, P.J. A. Smith, D. Thom. Biological interactions between polysaccharides and divalent cations: the egg-box model. *FEBS Lett*. 1973, *32*, 195-8.

46. G. Patel. Formulation/ Algae's functional excipent side. Available online at www.pharmaquality.com/ME2/Audiences/dirmod.aps. Issued February/ March 2006

47. O. Smidsrod, G. Skjak-Braek. Alginate as immobilization matrix for cells. *Trends in Biotechnology*. 1990, *8*, 71-78

48. A. Martisen, I. Storro, G. Skjak-Braek. Alginate as immobilization material: III. Diffusional properties. *Biotechnol Bioeng*.1992, *39*, 186-194

49. A. Omer, V. Duvivier-Kali, J. Fernandes, V. Tchipashvili, C.K. Colton, G.C. Weir. Long-term normoglycemia in rats receiving transplants with encapsulated islets. *Transplantation*. 2005, *79*, 52-58.

50. B. Thu, P. Bruheim, T. Espevik, O. Smidsrod, P. Soon-Shiong, G. Skjak-Braek. Alginate polycation microcapsules. II. Some functional properties. *Biomaterials*. 1996, *17*, 1069-1079.

51. H. J. Kong, D. Kaigler, K. KIm, D. J. Mooney. Controlling rigidity and degradation of alginate hydrogels via molecular weight distribution. *Biomacromolecules*. 2004, *5*, 1720-1727.

52. Y. A. Mùrch, I. Donati, B. L. Strand, G. Skjak-Brak. Effect of Ca 2+, Ba 2+, and Sr 2+ on alginate microbeads. *Biomacromolecules*. 2006, *7*, 1471-1480

53. A. Haug, O. Smidsrod. The effect of divalent metals on the properties of alginate solution. *Acta Chemica Scandinavica*. 1965, *19*, 341-351

54. M. S. Shoichet, R. H. Li, M. L. White, S. R. Winn. Stability of Hydrogels Used in Cell Encapsulation: An In Vitro Comparison of Alginate and Agarose. *Biotechnology and Bioengineering*. 1996, *50*, 374-381.

55. A.S. Michaels. Polyelectrolyte complexes. *Ind. Eng. Chem.* 1965, *57* (10), 32-40.

56. J. H. Hamman. Chitosan based polyelectrolyte complexes as potential carrier materials in drug delivery systems. *Mar. Drugs*. 2010, *8*, 1305-1322.

57. G. Decher, J. D. Hong, J. Schmitt. Buildup of ultrathin multilayer films by a self-assembly process: III. Consecutively alternating adsorption of anionic and cationic polyelectrolytes on charged surfaces. *Thin Solid Films*.1992, *210/211*, 831-835.

58. G. Decher, J. D. Hong. Buildup of ultrathin multilayer films by a self-assembly process.2. Consecutive adsorption of anionic and cationic bipolar amphiphiles and polyelectrolytes on charged surfaces. *Ber. Bunsen-Ges.* 1991, *95*, 1430-1434.

59. G. Decher. Fuzzy nanoassemblies: Toward layered polymeric multicomposites. *Science.* 1997, *277*, 1232-1237.

60. Z. Tang, Y. Wang, P. Podsiadlo, N. A. Kotov. Biomedical Applications of Layer-by-Layer Assembly: From Biomimetics to Tissue Engineering. *Advanced. Materials*. 2006, *18*, 3203-3224.

61. F. Lim, A. M. Sun. Microcapsulated islets as bioartificial endocrine pancreas. *Science* 1980, *210*, 908-910

62. P. de Vos, C. G. Hoogmoed, H. J. Busscher. Chemistry and biocompatibility of alginate-PLL capsules for immunoprotection of mammalian cells. *Journal of Biomedical Materials Research*. 2002, *60* (2), 252-259.

63. B. Dupuy, A. Arien, A. Perrot Minnot. FTIR of membranes made with alginate-polylysine complexes. Variations with mannuronic or guluronic content of the polysaccharides. *Art Cells Blood Subs Immob Biotech*. 1994, *22*, 71-82.

64. P. de Vos, B. De Haan . R. Van Schilfgaarde. Effect of the alginate composition on the biocompatibility of alginate-polylysine microcapsules. *Biomaterials*. 1997, *18*, 273-278.

65. P. Soon-Shiong, E. Feldman, R. Nelson, J. Komtebedde, O. Smidsrod, G. Skjak-Braek, T. Espevik, R. Heintz, M. Lee. Successful reversal of spontaneous diabetes in dogs by intraperitoneal microencapsulated islets. *Transplantation*. 1992, *54*(5), 769-74.

66. P. Soon-Shiong, R. Heintz, N. Merideth N, Q.X. Yao, Z. Yao, T. Zheng, M. Murphy, M.K. Moloney, M. Schmehl, M. Harris, R. Mendez, P.A. Sandford. Insulin independence in a type 1 diabetic patient after encapsulated islet transplantation. *Lancet*. 1994, *343*(8903), 950-951.

67. S. Darquy, M. E. Pueyo, F. Capron, G. Reach. Complement activation by alginate-polylysine microcapsules used for islet transplantation. *Artif Organs*. 1994; *18*(12), 898-903.

68. M. E. Pueyo , S. Darquy, F. Capron, G. Reach. In vitro activation of human macrophages by alginate-polylysine microcapsules. *J Biomater Sci Polym Ed*. 1993, *5*(3), 197-203.

69. B. L. Strand, L. Ryan, P. I. Veld, B. Kulseng, A. M. Rokstad, G. Skjak-Braek, K. Espevik T. Poly-L-lysine induces fibrosis on alginate microcapsules via the induction of cytokines. *Cell Transplant*. 2001, *10*(3), 263-75.

70. G. Orive, S. K. Tam, J. L. Pedraz, J. P. Halle. Biocompatibility of alginate–poly-L-lysine microcapsules for cell therapy. *Biomaterials*. 2006, *27*, 3691-3700.

71. S. K. Tam, J. Dusseault, S. Polizu, M. Menard, J. P. Halle, L. Yahia. Impact of residual contamination on the biofunctional properties of purified alginates used for cell encapsulation. *Biomaterials* 2006, *27*, 1296-1305.

72. J. Dusseault, G. Langlois, M. C. Meunier, M. Me´nard, C. Perreault, J. P. Halle. The effect of covalent cross-links between the membrane components of microcapsules on the dissemination of encapsulated malignant cells. *Biomaterials* 2008, *29,* 917-924

73. H. K. Holme,L. Davidsen, A. Kristiansen,O. Smidsroed. Kinetics and mechanisms of depolymerization of alginate and chitosan in aqueous solution. *Carbohydrate Polymers*. 2008, *73* (4), 656–664.

74. R. Li. Materials for immunoisolated cell transplantation. *Advanced Drug Delivery Reviews.* 1998, *33*, 87-109.

75. A. Murua, A. Portero, G. Orive, R. M. Hernandez, M. D. Castro, J. L. Pedraz. Cell microencapsulation technology: towards clinical application. *Journal of Controlled Release.* 2008, *132*, 76-83.

76. J. Dusseault, S. K. Tam, M. Menard, S. Polizu, G. Jourdan, L. Yahia, J. P. Halle. Evaluation of alginate purification methods: Effect on polyphenol, endotoxin, and protein contamination. *J. Biomed. Mater. Res. A*. 2006, *76*, 243-251

77. M. F. A. Goosen, G. M. O'Shea, H. M. Gharapetian, S. Chou, A. M. Sun. Optimization of microencapsulation parameters: semipermeable microcapsules as a bioartificial pancreas. *Biotechnol. Bioeng*. 1985, *27*, 146-150.

78. A. Greimel, M. Werle, A. Bernkop-Schnürch. Oral peptide delivery: in-vitro evaluation of thiolated alginate/poly (acrylic acid) microparticles. *Journal of Pharmacy and Pharmacology*. 2007, *59*, 1191-1198.

79. A. Bernkop-Schnürch. Thiomers: A new generation of mucoadhesive polymers. *Advanced Drug Delivery Reviews*. 2005, *57*, 1569– 1582.

80. M. Davidovich-Pinhas, O. Harari, H. Bianco-Peled. Evaluating the mucoadhesive properties of drug delivery systems based on hydrated thiolated alginate. *Journal of Controlled Release*. 2009, *136*, 38–44.

81. A. I. Chou, S. B. Nicoll. Characterization of photocrosslinked alginate hydrogels for nucleus pulposus cell encapsulation. *Journal of Biomedical Materials Research Part A*. 2009, *91A* (1), 187-194.

82. Q. Jeon, K. H. Bouhadir, J. M. Mansour, E. Alsberg. Photocrosslinked alginate hydrogels with tunable biodegradation rates and mechanical properties. *Biomaterials*. 2009, *30*, 2724–2734.

83. A. M. Rokstad, I. Donati, M. Borgogna, J. Oberholzer, B.L. Strand, T. Espevik, G. Skjak-Braek. Cell-compatible covalently reinforced beads obtained from a chemoenzymatically engineered alginate. *Biomaterials*. 2006, *27*, 4726–4737.

84. I. Donati, K. I. Draget, M. Borgogna, S. Paoletti, G. Skjak-Brnk. Tailor-Made Alginate Bearing Galactose Moieties on Mannuronic Residues: Selective Modification Achieved by a Chemoenzymatic Strategy. *Biomacromolecules*. 2005, *6*, 88-98.

85. F. Cellesi, N. Tirelli, J. A. Hubbell. Materials for cell encapsulation via a new tandem approach combining reverse thermal gelation and covalent crosslinking. *Macromolecular Chemistry and Physics*. 2002, *203* (10/11), 1466-1472.

86. M. Z. Lu, H. L. Lan, F. F. Wang, S. J. Chang, Y. J. Wang. Cell encapsulation with alginate and α-phenoxycinnamylidene-acetylated poly (Allylamine).*Biotechnology and Bioengineering*. 2000, *70* (5), 479-483.

87. M. A. Gauthier, M. I. Gibson, H. A. Klok. Synthesis of functional polymers by post-polymerization modification. *Angew. Chem. Int. Ed.* 2009, *48*, 48-58.

88. M. A. Gauthier, H. A. Klok. Peptide/protein–polymer conjugates: synthetic strategies and design concepts. *Chem. Commun.* 2008, *23*, 2591-2611.

89. M. A. J. Mazumder, F. Shen, N. A. D. Burke, M. A. Potter, H. D. H. Stover. Self-cross-linking polyelectrolyte complexes for therapeutic cell encapsulation. *Biomacromolecules*. 2008, *9*, 2292–2300.

90. Mechanically Enhanced Microcapsules for Cellular Gene Therapy. F. Shen, M. A. J. Mazumder, N. A. D. Burke, H. D. H. Stover, M. A. Potter. *Journal of Biomedical Materials Research Part B: Applied Biomaterials*. 2009, *90* (1), 350-361.

91. M. A. J. Mazumder, N. A. D. Burke, F. Shen, M. A. Potter, H. D. H. Stver. Core-crosslinked alginate microcapsules for cell encapsulation. *Biomaterials*, 2009, *10* (6), 1365-1373.

92. P. J.A. Gemink , L. van Dalen, L. G. J. van der Ven, Richard R. Lamping. Analytical aspects and film properties of two-pack acetoacetate functional latexes. *Progress in Organic Coatings*, 1996, *27*, 73-78.

93. R. J. Esser, J. E. Devona, D. E. Setzke, L. Wagemans. Waterbased crosslinkable surface coating. *Progress in Organic Coatings*, 1999, *36*. 45-52.

94. I. Gonzalez, G. Arzamendi, J. M. Asua, J. R. Leiza. Unexpected crosslinking during acetoacetoxy group protection on waterborne crosslinkable latexes. *Macromolecular Materials and Engineering*, 2006, *291*, 1185-93.

95. T. Nishihata, J. Kato, K. H, Kim, M. Kobayashi, I. Kitagawa, A. Kamada. Formation and hydrolysis of enamine in aqueous solution. *Chem. Pharm.Bull*, 1984, *32* (11), 4545-50.

96. J. P. Guthrie, F. Jordan. Enamine formation and hydrolysis. Ethyl 6–cyanomethylaminocrotonate. *Journal of the American Chemical Society*, 1972, *94* (26), 9132-36.

97. J. V. M. Weaver, I. Bannister, K. L. Robinson, X. Bories-Azeau, and S. P. Armes. Stimulus-Responsive Water-Soluble Polymers Based on 2-Hydroxyethyl Methacrylate. *Macromolecules,* 2004, *37*, 2395-2403.

98. A. Stammati, F. Zampaglioni, F. Zucco. Furaltadone cytotoxicity on three cell lines in the presence or absence of DMSO: Comparison with furazolidone. *Cell Biology and Toxicology*. 1997, *13*, 125-130.

99. E. Watanabe, R. Sudo, M. Takahashi, M. Hayashi. Evaluation of absorbability of poorly water-soluble drugs: validity of the use of additives, *Biol. Pharm. Bull*, 2000, *23*, 838-43.

100. G. Da Violante, N. Zerrouk, I. Richard, G. Provot, J. C. Chaumeil, P. Arnaud.Evaluation of the cytotoxicity effect of dimethyl sulfoxide (DMSO) on Caco2/TC7 colon tumor cell cultures. *Biol. Pharm. Bull*. 2002, *25*(12), 1600-1603.

101. A. G. Sanchez, M. T. Aldave. Proton magnetic resonance spectra of N-substituted 3-aminocrotonic esters. *J. Chem. Soc (c).* 1968, 2570-73.

102. F. Tanaka, R. Thayumanavan, N. Mase, C. F. Barbas. Rapid analysis of solvent effects on enamine formation by fluorescence: how might enzymes facilitate enamine chemistry with primary amines? *Tetrahedron Letters*, 2004, *45*, 325–28.

103. T. Roberts, U. De Boni, M.V. Sefton. Dopamine secretion by PC12 cells microencapsulate in a hydroxyethyl methacrylate-methyl methacrylate copolymer. *Biomaterials*, 1996, *17*, 267-275.

104. P. Matricardi, M. Pontoriero, T. Coviello, M. A. Casadei, F. Alhaique. In situ cross-linkable novel alginate-dextran methacrylate IPN hydrogels for biomedical applications: mechanical characterization and drug delivery properties. *Biomacromolecules*, 2008, *9*, 2014–2020.

105. L. Baruch, M. Machluf. Alginate–chitosan complex coacervation for cell encapsulation: effect on mechanical properties and on long-term viability. *Biopolymers*, 2006, *82*, 570–579.

106. J. Kadokawa, S. Saitou, S. Shoda. Preparation of alginate-polymethacrylate hybrid material by radical polymerization of cationic methacrylate monomer in the presence of sodium alginate. *Carbohydrate Polymers*, 2005, *60*, 253–258.

107. T. Coradin, N. Nassif, J. Livage. Silica–alginate composites for microencapsulation. *Appl Microbiol Biotechnol*, 2003, *61*, 429–434.

108. T. Araki, A. P. Hitchcock, F. Shen, P. L. Chang, M. Wang, R.F. Childs. Quantitative chemical mapping of sodium acrylate- and N-vinylpyrrolidone-enhanced alginate microcapsules. *J. Biomater. Sci. Polymer Edn*, 2005, *16* (5), 611-627.

109. Product Information Bulletin of NovaMatrix/FMC Corporation.

110. C. M. Gardner, N. A. D. Burke, T. Chu, F. Shen, M. A. Potter, H. D. H. Stöver. Poly (methyl vinyl ether-alt-maleic acid) Polymers for Cell Encapsulation. *Journal of Biomaterials Science,* 2010, DOI: 10.1163/092050610X535149.

111. M. R. Klugerman. Chemical and physical variables affecting the properties of fluorescein isothiocyanate and its protein conjugates. *The Journal of Immunology*, 1965, *95* (6), 1165-1173.

112. E. Pobozy, W. Czarkowska, M. Trojanowicz. Determination of amino acids in saliva using capillary electrophoresis with fluorimetric detection. *J. Biochem. Biophys. Methods*, 2006, *67*, 37–47.

113. S. K. Lau, F. Zaccardo, M. Little, P. Banks. Nanomolar derivatizations with 5-carboxyfluorescein succinimidyl ester for fluorescence detection in capillary electrophoresis. *Journal of Chromatography A*, 1998, *809*, 203–210.

114. B. Thu, O. Gåserød, D. Paus, A. Mikkelsen, G. Skjak-Bræk, R. Toffanin, F. Vittur. R. Rizzo. Inhomogeneous alginate gel spheres: an assessment of the polymer gradients by synchrotron radiation induced X-Ray emission, magnetic resonance microimaging, and mathematical modeling. *Biopolymers*, 2000, *53*, 60-71.

115. N. M. Velings. M. M. Mestdagh. Physico-chemical properties of alginate gel beads. *Polymer Gels and Networks*, 1995, *3*, 311-330.

116. M. A. J. Mazumder, Polyelectrolytes for therapeutic cell encapsulation. *Ph. D. Thesis, McMaster University*, 2009.

117. H. Bysell, M. Malmsten. Visualizing the Interaction between Poly-L-lysine and Poly (acrylic acid) Microgels Using Microscopy Techniques: Effect of Electrostatics and Peptide Size. *Langmuir*, 2006, *22*, 5476- 5484.

118. S. E. Burke, C. J. Barrett. pH-Responsive Properties of Multilayered Poly(L-lysine)/ Hyaluronic Acid Surfaces. *Biomacromolecules*, 2003, *4*, 1773-1783.

119. O. Gåserød, O. Smidsrød, G. Skjåk-Bræk. Microcapsules of alginate-chitosan. I. A quantitative study of the interaction between alginate and chitosan. *Biomaterials*, 1998, *19*, 1815-1825.

120. O. Gåserød, A. Sannes, G. Skjåk-Bræk. Microcapsules of alginate-chitosan. II. A study of capsule stability and permeability. *Biomaterials*, 1999, *20*,773-783.

121. A. Martinsen, I. Storrø, G. Skjåk-Bræk. Alginate as immobilization material- III. Diffusional properties. *Biotechnol Bioeng*, 1992, *39*,186-194.

122. A. M. Rokstad, I. Donati, M. Borgogna, J. Oberholzer, B. L. Strand, T. Espevik, G. Skjak-Braek. Cell-compatible covalently reinforced beads obtained from a chemoenzymatically engineered alginate. *Biomaterials*, 2006, *27*, 4726–4737.